

Manuscript Details

Manuscript number	IRBM_2018_191_R1
Title	Effect of the photodynamic therapy applications with potent microalgae constituents on several types of tumor
Article type	Original article

Abstract

Background In recent years, microalgae (MA) have attracted much interest considering their possible therapeutic application. They contain active natural compounds or derivatives (extracts, pure or chemically modified compounds) that have increasing applications in the pharmaceutical industry. **Methods** The present study aims to examine microalgae for new photosensitizers, with a potential to be used in the light-associated treatment of tumors. Semi-purified extracts of several microalgae strains were evaluated as photosensitizers for photodynamic therapy (PDT) applications. Four tumor cell lines (A549, LNCap, MCF-7, and MDA-MB 435) were used to assess 34 samples extracted by three methods: cellulase enzyme, lysozyme enzyme and ultra-sonication. The fluorescence measurements and the recorded images alongside the spectral intensities between 650- 800 nm wavelengths provided characteristic features to some of the contents of the examined extracts. **Results** Several microalgae constituents activated by blue light (BL), red light (RL) or both (in sequence) exhibited significant effects on the viability of the tumor cell lines, decreasing it as much as 95 % for certain MA constituents. Majority of the MA constituents showed a higher phototoxicity after exposure to both blue and red lights than the photo-induced toxicity when exposed to a single light source. The viability of the tumor cells exhibited the dose dependent response with the MA constituents. **Conclusion** The results clearly showed that MA constituents are potential photosensitizers that have a significant photo-damage effects on the tested cancer cells.

Keywords	Microalgae; Anticancer agent; Photodynamic therapy; Photosensitizers; Enzymatic extraction
Taxonomy	Biomaterials, Biochemical Engineering
Corresponding Author	Sulaiman Al-Zuhair
Corresponding Author's Institution	UAE University
Order of Authors	Asma Jabeen, Brandon Reeder, Dimitri Svistunenko, Soleiman Hisaindee, Salman Ashraf, Sulaiman Al-Zuhair, sinan battah
Suggested reviewers	Haq Nawaz Bhatti, Rania Hallaq, Paul Hamilton

Effect of the photodynamic therapy applications with potent microalgae constituents on several types of tumor

Asma Jabeen ¹, Brandon Reeder ¹, Dimitri Svistunenko ¹, Soleiman Hisaindee ², Salman Ashraf ², Sulaiman Al-Zuhair ^{3*}, Sinan Battah^{1*}

¹ The School of Biological Sciences, University of Essex, Colchester, CO4 3SQ, UK

² Chemistry Department, College of Science, UAE University, 15551 Al-Ain, UAE

³ Chemical Engineering Department, College of Engineering, UAE University, 15551 Al-Ain, UAE

* Corresponding authors: s.alzuhair@uaeu.ac.ae and sbhatt@essex.ac.u

Highlights

- Semi-purified extracts of several microalgae strains were evaluated as photosensitizers
- Photodynamic therapy (PDT) was tested on four tumor cell lines (A549, LNCap, MCF-7, and MDA-MB 435)
- Extracts from cellulase, lysozyme and ultra-sonication treated MA cells were examined.
- By treatment with MA constituents, viability of tumor cell lines decreased by up to 95% with light activation.
- Majority of the MA constituents showed a higher phototoxicity after exposure to both blue and red lights.

Abstract

Background

In recent years, microalgae (MA) have attracted much interest considering their possible therapeutic application. They contain active natural compounds or derivatives (extracts, pure or chemically modified compounds) that have increasing applications in the pharmaceutical industry.

Methods

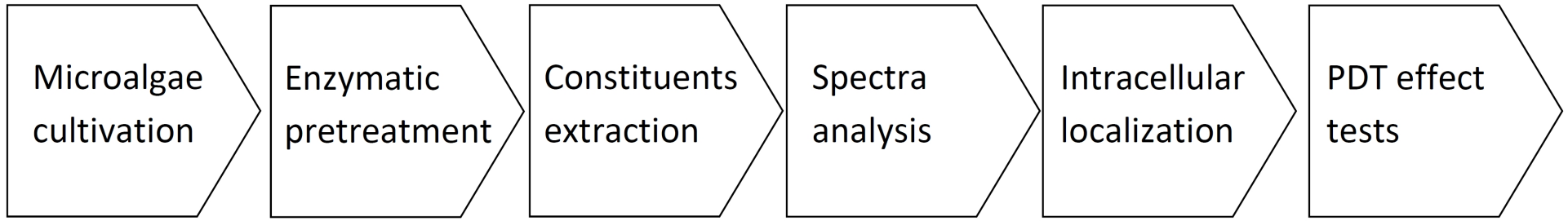
The present study aims to examine microalgae for new photosensitizers, with a potential to be used in the light-associated treatment of tumors. Semi-purified extracts of several microalgae strains were evaluated as photosensitizers for photodynamic therapy (PDT) applications. Four tumor cell lines (A549, LNCap, MCF-7, and MDA-MB 435) were used to assess 34 samples extracted by three methods: cellulase enzyme, lysozyme enzyme and ultra-sonication. The fluorescence measurements and the recorded images alongside the spectral intensities between 650- 800 nm wavelengths provided characteristic features to some of the contents of the examined extracts.

Results

Several microalgae constituents activated by blue light (BL), red light (RL) or both (in sequence) exhibited significant effects on the viability of the tumor cell lines, decreasing it as much as 95 % for certain MA constituents. Majority of the MA constituents showed a higher phototoxicity after exposure to both blue and red lights than the photo-induced toxicity when exposed to a single light source. The viability of the tumor cells exhibited the dose dependent response with the MA constituents.

Conclusion

The results clearly showed that MA constituents are potential photosensitizers that have a significant photo-damage effects on the tested cancer cells.



Effect of the photodynamic therapy applications with potent microalgae constituents on several types of tumor

Abstract

Background

In recent years, microalgae (MA) have attracted much interest considering their possible therapeutic application. They contain active natural compounds or derivatives (extracts, pure or chemically modified compounds) that have increasing applications in the pharmaceutical industry.

Methods

The present study aims to examine microalgae for new photosensitizers, with a potential to be used in the light-associated treatment of tumors. Semi-purified extracts of several microalgae strains were evaluated as photosensitizers for photodynamic therapy (PDT) applications. Four tumor cell lines (A549, LNCap, MCF-7, and MDA-MB 435) were used to assess 34 samples extracted by three methods: cellulase enzyme, lysozyme enzyme and ultra-sonication. The fluorescence measurements and the recorded images alongside the spectral intensities between 650- 800 nm wavelengths provided characteristic features to some of the contents of the examined extracts.

Results

Several microalgae constituents activated by blue light (BL), red light (RL) or both (in sequence) exhibited significant effects on the viability of the tumor cell lines, decreasing it as much as 95 % for certain MA constituents. Majority of the MA constituents showed a higher phototoxicity after exposure to both blue and red lights than the photo-induced toxicity when

exposed to a single light source. The viability of the tumor cells exhibited the dose dependent response with the MA constituents.

Conclusion

The results clearly showed that MA constituents are potential photosensitizers that have a significant photo-damage effects on the tested cancer cells.

Keywords

Microalgae; Anticancer agent; Photodynamic therapy; Photosensitizers; Enzymatic extraction

Introduction

Drug resistance is still a major obstacle in the effective chemotherapeutic treatment of cancer, despite numerous efforts to overcome these problems [1, 2]. Cancer incidences are increasing and therefore effective therapeutic approaches are needed to combat these malignancies [1].

Recent data highlight the steps of deregulated cellular proliferation, metastasis and apoptosis [2, 3]. In recent years, the study of the chemistry of microalgae has seen a tremendous increase due to the need for pharmaceutical applications of potentially bioactive compounds [4]. Algae extracts are documented to have anti-cancer activity in vitro and in vivo and induce growth inhibition in cancer cells while leaving the non-transformed cells intact [5].

The major interest in microalgae is the capacity to modulate their metabolism according to environmental conditions. Moreover, microalgae are acknowledged to be a diverse source of bioactive molecules that play physiological roles in the organisms [6, 7]. Marine algae, including the microalgae, are considered to be a major source of novel natural bioactive substances, making them attractive for development by the pharmaceutical sectors [8]. There are polysaccharides, protein, peptides, or unsaturated long chain fatty acids in microalgae that have chemical structures not found in other natural sources, or which are present at much higher concentrations [9]. Several compounds in the algae's pigments have attracted high

levels of interest, such as β carotene, astaxanthin, phycoerythrin, and tetrapyrrole [10, 11]. Some compounds produced by algae (and the microalgae, in particular) can respond with a remarkable selectivity to a wide diversity of molecular targets. (i.e. inhibitors for specific enzyme of a particular pathway for tumor proliferation). A variety of red algae as well as that of the brown algae (Phaeophyceae) have anti proliferative and anti-inflammatory activities [12, 13]. The in vivo and in vitro studies of the seaweed constituents reported the antimutagenic mechanisms and potential anticarcinogenic effects of kelp and red algae against colon and breast cancers [14]. An aqueous extract of *G. corticata* showed cytotoxic activity against leukemic cell lines Jurkat and Molt-4 [15]. Many of those pigments are photosensitive and fluorescent. Development of the fluorescent protein family to include optical highlighters and fluorescence resonance energy transfer (FRET) biosensors further equips this abundant class of fluorophores with biological probes efficient for photoactivation, photoconversion, and detection of molecular interactions beyond the resolution limits of optical microscopy [16]. Keeping in mind that some of the modified fluorescent proteins based on the fundamental chromophore structure present in green fluorescent protein could not only emit fluorescence, but also produce Reactive Oxygen Species (ROS) upon excitation with light such as KillerRed [17]. The species such as singlet oxygen or free radicals have destructive impact when they are generated within a tumour tissue, particularly in photodynamic therapy applications (PDT). PDT is an alternative treatment for cancer that involves administration of a photosensitive drug or PS that localizes at the tumor tissue followed by in situ excitation at an appropriate wavelength of light. PDT is commonly practiced in the treatment of several cancers, including those in the head & neck, lungs, bladder and particularly skin cancers [18, 19]. It has also been successfully used in the treatment of non-cancerous conditions such as age-related macular degeneration (AMD) [20], psoriasis [21] and atherosclerosis [22]. In addition, PDT has shown some

efficacy in anti-viral treatments of such conditions as herpes [23]. Unlike traditional methods such as chemotherapy and radiotherapy, PDT allows a relatively higher degree of specificity by targeting malignant and pre-malignant cells. It is also preferred when surgical removal is considered risky in certain cases such as oesophageal [24] and brain tumors [25, 26].

There have been few studies on combinations of PDT with standard antitumor regimens; PDT can be used in combination with surgery as a neoadjuvant, adjuvant or repetitive adjuvant treatment, preferably fluorescence image-guided technique that confine illumination to the lesions [19]. Microalgae remain, to date, largely unexplored and unexploited. It represents a unique opportunity to obtain novel photosensitizers (PSs) from the naturally occurring pigment fractions, which can be exploited for PDT. Therefore, several semi-purified extracts from different microalgae have been assessed with two cancer cell lines in this study, In the light of persistent demands to develop new PSs to fulfill a professed need in PDT drug's array. To our knowledge, this is the first time a wide range of MA constituents have been examined in PDT field, evaluating their activities against tumor cell lines. The results of this study will provide the starting points for drug design and to understand the role of a chemical in advanced strategic PDT technology. We aimed at identifying potentially active fractions/extracts, their isolation and identification of novel candidates.

Materials and Methods

Materials

The extracts of microalgae (MA) were solid materials, some of the samples were off white powder and others were green pigments. The samples were divided into three categories, depending on their methods of extracting which were described in our previous publication [27]. The three Categories were Category I, MA constituents from cellulase treated samples, (odd numbers, MA-1 to MA-23). Category II; MA constituents from lysozyme treated

samples of MA, (even numbers MA-2 to MA-24), and Category III; MA constituents from ultra-sonication treated MA, (MA-25 to MA-31).

[Table 1]

Chemical treatment for MA green dye samples

In order to activate the green pigments constituents that has metal ions such as chlorophylls and tetrapyrroles compounds, it was necessary to remove the coordinating metal (magnesium or zinc) within the cavity of their structures. The green pigments (Category III samples) were dissolved in 50 % aqueous Dimethyl Sulfoxide (DMSO) treated with 5 M hydrochloric acid. The samples were stirred at room temperature for 24 h, dialyzed for 24 h against pure water in dialysis membrane tubes (Cellulose Membrane, Fisher, UK) with 100 Dalton Cut-off, then were freeze dried (-80 °C). The stock solutions of the solid materials were dissolved in ultra-pure water or DMSO (for the slightly insoluble materials in water, with concentration 100 mg of dry weight per ml, therefore DMSO concentration in the cell culture medium didn't exceed more than 1 %).

Spectral analysis

The absorbance spectra of all samples (dissolved in water, 20 µg/mL for Category I & II and 5 µg/ml for category III) were recorded in cells free medium using diode array spectrophotometer (Agilent 8453, UK) between the wavelengths of 220 and 850 nm with exit slot 10.

Cell culture preparations

The anticancer activities of the MA constituents were evaluated against two of the most common human tumour cell lines using PDT techniques. Cell lines of A549 (human lung carcinoma), MCF-7 (human breast adenocarcinoma) were cultured in Dulbecco's Modified Eagle Medium (DMEM). The medium were mixed in L-glutamine (20 IM) and phenol red,

and supplemented with 10 % fetal bovine serum (FBS), gentamycine (500 units/mL; Life Technologies). The cells were grown as monolayers in sterile, vented-capped, angle-necked cell culture flasks (Corning) and were maintained at 37 °C in a humidified 5% CO₂ incubator (IR Autoflow Water-Jacketed Incubator; JenconsNuaire) until confluent.

Fluorescence measurement

All MA extracts were checked for their fluorescence properties in A549 and MCF-7; cells were seeded into 96-well plates in triplicates at a density between $5-8 \times 10^4$ per well. Following incubation for 48h, the cells were washed with phosphate buffer saline (PBS) and 100µl solutions containing each sample at a concentration range of 100 µg/mL to 500 µg/mL or to 1000 µg/mL (as specified in the legends under the graphs) were prepared in DMEM medium and added to their designated wells. Each well plate contained three control wells without MA constituents. Also, one plate contained Pc-al as a reference with 150 µM ($\approx 86 \mu\text{g/mL}$). The plates were wrapped with aluminum foil to avoid the exposure to any light and the cells were incubated for 24 h at 37 °C in 5 % CO₂ incubator. The medium was then discarded and the cells were washed twice with PBS to remove any excess of materials. MA fluorescent constituents were excited at wavelength 395 nm and the spectra of MA fluorescence emissions recorded between wavelengths of 600–850 nm. The intracellular fluorescence emission intensity was measured at wavelength 670 nm after excitation at wavelength 395 nm with fluorescence plate reader spectrophotometer (MR 700 Dynatech, Dynex, USA).

Fluorescence microscopic imaging

The cell line A549 was cultured with MA constituents as described above. Treated cells were covered with foil to protect from light. After 24 h incubation, the excess of MA samples in the culture medium was discarded. The cells were then washed twice with PBS and phenol

red free culture medium was added for the live cell's fluorescence imaging. a Nikon A1 si Confocal microscope (Nikon, Tokyo, Japan model, UK) was used for imaging, with 20x objective, and laser settings were as follows; red channel 1, excitation wavelength 398.7 nm, emission wavelength 700 nm and red channel 2, excitation wavelength 560.5 nm, emission wavelength 595 nm. Sequential laser scanning was used to avoid the bleed through between the channels. Nikon NIS Elements software version 3.21.03 (Nikon, Tokyo, Japan) was employed for image processing.

Photodynamic treatment (PDT)

The photocytotoxicity of the cells was determined using the 3-(4,5-dimethylthiazol-2-yl)-2,5-diphenyltetrazolium bromide (MTT) assay. Cells were seeded into 96-well plates in triplicates at a density between $5-8 \times 10^4$ per well as above. Following incubation for 48 h, the cells were washed with PBS and 100 μ l solutions containing each sample at a concentration of between 100 and 500 μ g/mL or 1000 μ g/mL (according to each set of conditions for the experiment) were added to their designated wells. Each well plate contained minimum of three control wells without MA constituents and exposed to the same environment of the cells with MA constituents. Each experiment also contained the PS, Aluminum-phthalocyanine chloride (Pc-AL) with a concentration of 50 μ M, 100 μ M, and 150 μ M as a reference compound. The plates were wrapped with aluminum foil to avoid the exposure to any light and the cells were incubated for 24 h at 37 °C in 5% CO₂ incubator. The cells were washed with PBS to remove the excess of the samples and replaced by fresh full medium. The plates were irradiated with LED blue light (BL) and red light (RL) sources (Phantom, Shenzhen CIDLY Optoelectronic Technology, China), equipped with a fan to eliminate any heat and emit a uniform field of low-power, LED (75 W). The BL and RL sources were fixed within 30 cm distance from the top of the cell culture plates in a black box. The PDT experiments were carried out using three different separate assays; BL for 5 min, RL for 5 min, and 5 min

BL followed by 5 min RL, then incubated for 18 h at 37 °C in 5 % CO₂ incubator. To measure the phototoxicity, cells were incubated with the medium containing MTT (0.5 mg/mL dissolved in full medium) for 1 h. The insoluble end product (formazan derivatives) was dissolved in 100 µL DMSO after removing the medium. UV absorption was quantified at 550 nm using a 96-well plate reader (MR 700 Dynatech, Dynex). The means of cell survival (viabilities) were calculated for each sample and expressed as a percentage of control (cells without the samples).

MA concentration dependency effect on the phototoxicity and IC₅₀ determination

To examine the relationship between the concentration of MA samples and the phototoxicity, a range of concentrations were optimized and assessed. Cells were seeded and treated as above with a range of concentrations. According to their PDT efficacy, the concentrations for Category I and II were between 200 to 1000 µg/mL, whereas, Category III were between 20 to 100 µg/mL. The cell's viability were calculated as percentages of control (cells without MA treatment). The values MA concentrations of that exhibited 50 % cell death (IC₅₀) were determined for the most effective samples from each Category

Cytotoxicity evaluation

The cytotoxicity “dark toxicity” of all MA constituents was examined in A549 and MCF-7 cell lines to evaluate the intrinsic chemical toxicity of MA samples. Well plates were prepared in the same manner as above but without irradiation. The cells were incubated with the samples with the highest concentration for each category (1000 µg/mL for Category I and II and 100 µg/mL for Category III). The plates were kept in darkness all the time by wrapping the plates with aluminum foil and incubated at 37 °C in 5 % CO₂ incubator for 24 h. Cells were then washed and they were subjected to the MTT assay. The viabilities of the cells were

calculated as percentages of control (untreated cell with MA constituents from the same plate).

Statistics

Each experiment was repeated mostly in triplicates at different dates. The presented results are the average of the repeated experiments minimum of three different days to ensure reproducibility, with error bars representing the standard deviations. The t-test statistic for each experiment was carried out and $p < 0.05$ considered significant.

Results

The search for bioactive antitumour agents from microalgae requires varieties of the metabolite compositions of the algae extracts. Application of different extraction's techniques should provide different groups of chemicals, each group sharing some common constituents in variable quantities. The sources of biological extracts were obtained seven microalgae species with three methods of extracts. The details of extractions were previously published and our objective here to identify the most bioactive and photosensitive extracts to be isolated and developed later for photodynamic therapy (PDT) applications.

Spectral analysis of MA constituents

The data analysis of the absorption spectra for some of the tested categories demonstrated the existence of the naturally occurring phenolic and flavonoids groups [28, 29]. The absorbance spectra for MA constituents were recorded in water (cell free medium) for all the extracts to provide the first insight of the components contained in the samples. The majority of MA constituents from all the above categories displayed high absorbance peaks at wavelength between 220-300 nm, 400-500 nm and another peak between 650–750 nm, (Figure 1-A, -B, and -C). MA Constituents exhibited absorbance intensity variations reflecting their characteristic chemical components. Only MA-09, -15, and -17 from Category

1, MA-2, -8, -10, -16, -18, and -20 from Category II, and MA-25 to MA-31 from Category III have variable absorbance intensities at all the above region peaked at around 670 nm. The spectra analysis Category III showed some characteristic features of the tetrapyrroles compounds, particularly chlorins, where the Soret bands appeared around 400 nm and Q bands between 630 – 800 nm [29]. The rest of MA samples have much weaker absorbance due to some aggregation in water.

[Figure 1]

Biological evaluation

The evaluation of MA extracts was conducted first in two of the most common human tumour cell lines A549 and MCF7. Further two cell lines LNCap (human prostate cells derived from metastatic site lymph node) and MDA MB-435 (human breast adenocarcinoma) were employed in some experiments in order to check the specificity of the cell type and the capability of MA for each type. A fluorescence analysis for all MA constituents was conducted in all tumor cell lines between 600 to 800 nm wavelengths. The emission spectrum of MA samples in A549 cell line presented in Fig 2-A, -B, and -C displayed inherent fluorescence features. The emission spectra of fluorescent MA constituents provided considerable fluorescence traces for some samples of Category I (MA-09, -15, -17), Category II (MA-02, -16, -20), and Category III (MA-25 to MA-31) in the red region of the light spectrum between the wavelength 650–800 nm in A549 selected data are presented in Fig 2, A, B, and C. In our experimental setting, it wasn't possible to measure the fluorescence below 600 nm wavelength due to the large background of the 96 well plates.

[Figure 2]

Fluorescence intensities of the samples that showed fluorescent ability of MA samples were measured at ($\lambda_{\text{excitation}}$ 400 nm and $\lambda_{\text{emission}}$ 670 nm) in the tumor cell lines including A549 cell

line and MCF-7 cell lines (Fig 3-A and -B) to give an indication regarding the fluorescent materials and their expected phototoxicity. MA Constituents (MA-7, -11, -19 and -23) had very weakly fluorescence emission, whereas MA-01, 03, -05, -13, and -21 did not show detectable levels of fluorescence at 670 nm wavelength. The samples in Category I (MA-09, -15, -17) showed the highest fluorescence intensity of that group (between \approx 100 -250 units). However, the fluorescence capacities of MA-16, -18, and -20 from Category II and the reference compound Pc-al were much higher than those in Category I in the magnitude of 3-4 folds (between \approx 250 to 950 units). This data also reflects MA constituent's uptake specificity by cell lines, in particular MCF-7 showed significantly higher uptake of MA-09, whereas MA-15 and -17 were absorbed by A549 more than MCF-7 cell line. MA-16 (\approx 950 units), -18 (\approx 380 units) -20 (\approx 480 units) and Pc-al (\approx 400 units) were strongly fluorescent reflecting their higher cellular uptake by A549 cell line as compared to MCF-7 cell line (\approx 600, 180, 280, and 350 units, respectively). Samples MA-02, -04, -08 and -10 were moderately fluorescent, whereas MA-12 and -24 were very weakly fluorescent.

[Figure 3]

A dose dependence profile for the fluorescence emissions of MA constituents, Category II (ultra-sonication extracts) in MCF-7 and A549 cells were examined and presented in A549 and MCF-7 (Figure 4-A and -B, respectively) as an example of the strongly fluorescent materials. The fluorescence intensities exhibited positive correlation against a range of concentrations (100–500 μ g/mL) for MA-25, -26, -27, and -28 and MCF-7 (Fig 4-B) cell lines. The Pearson correlation, determined between the incubated MA constituents doses and the fluorescence signals, was larger than 0.92 in all the samples and both cell lines.

[Figure 4]

Intracellular localization

Fluorescence microscopy has been extensively used to investigate the micro-distribution and detailed examination of drug deposition in cells and tumor tissue. In this study, several MA constituents, with potential PSs, are imaged by confocal microscopy in the A549 cell line. Figure 5 presented as an example to confirm the identity and the existence of the fluorescent materials within the cellular compartments. Imaging data shows that the PSs can readily pass through the plasma membrane and mostly accumulated in the cytoplasmic region. Grey images are the differential interference contrast (DIC) of the cells. The fluorescence was exhibited by the PSs overlaid to indicate both the red fluorescence and the contrast images. All the imaging data were recorded using constant laser power and gain that was initially adjusted according to untreated control. Untreated control cellular images did not show red fluorescence thus no significant auto-fluorescence was detected in A549 cell line (Figure 5) and LNCap cells (Supporting Data, Figure S-1). Among microalgae samples, highest cellular uptake and strongest fluorescence in red channel were pronounced with MA 02, -16, -18, -30, and -31, whereas MA -09, -15, and -17, appeared moderately fluorescent. All MA constituents that demonstrated strong fluorescence in the cytoplasmic region did not seem to display much of the fluorescent signals in the nuclei. The results coincide with the fluorescence intensity profiles of the same samples in Figs 2, 3, and 4.

[Figure 5]

PDT effect of MA constituents on tumour cell lines

The phototoxic effect of MA constituents was assessed on the viability of four tumor cell lines after activation of the potential PSs within the samples with three techniques using two light sources, BL, RL or both light in sequence (5 min each).

PDT of MA constituents with BL

MA constituents of Category I and II were assessed for their photocytotoxicity on A549 and MCF-7 cell's viability. Both categories showed different quantities of fluorescence in green and red regions of the light spectrum. Therefore, following the treatment with MA constituents for 24 h, cell lines were irradiated with BL for 5 min after optimizing the time of exposure. The cell survival of categories (I) and (II) of MA constituents represented as percentages of the control (untreated cells) upon BL activation is shown in Figure 6-A and -B, respectively. MA constituents; MA-03, -05, 09, -15 and -17 caused \approx 60-80% cell death in A549 and MCF-7 cell line. In Category I samples, MA -09 appeared to be the best candidate against all cancer cell lines used from the cellulase extracted groups. MA constituents; MA-02, -16, -18, -20 caused \approx 67% phototoxicity in A549 and, while MA-02, -04, -06, -08, -10, -16, -18, and -20 exhibited significant phototoxicity between \approx 4 –84 % in MCF-7 cell lines, with the most deleterious effect caused by MA-02 and -18.. Thus MA constituents showed selective efficacy towards cancer cell lines. Further 5 min BL exposure didn't show extra significant effect on the above MA samples. Also, the phototoxic effect of the above samples that were activated by BL and evaluated against two other cell lines LNCap and MDA MB-435 showed also specificity towards cell lines (Supporting Data, Figure S-2).

[Figure 6]

PDT of MA constituents with RL

The photocytotoxic effects of categories I, II, and III samples on the viability of A549 and MCF-7 cells after irradiation with RL for 10 min illustrated in Figure 7-A, B and C, respectively. The viability of the cells was compared with untreated control group and with the reference drug (aluminum-phthalocyanine chloride (AlPc, PS used as an anticancer agent for PDT). The phototoxicity effect of some of Category I (MA-09, -15, and -17) caused \approx 60-85% cell death in both cell lines, A549 and MCF-7. Therefore, photodamaging efficacy of

Category I (cellulase treated samples) was improved slightly when activated with RL. In contrast, Category II (Lysozyme treated samples) did not show significant difference between blue and RL activation (Figure 7-B). PDT effects of Category III samples (ultra-sonication extracts, clear green pigments) were also assessed in response to RL irradiation displayed high fluorescence features in A549 and MCF-7 cell lines (Figure 7-C). The data indicated selective efficacy of MA constituents towards cancer cell line types after 5 min exposure. The samples (MA-25, -26, -28, -29, and -31) induced cell death up to $\approx 95\%$ in A549 and 90% in MCF-7. The samples (MA-30) lead to $\approx 84\%$ phototoxicity in A549 and 24% in MCF-7 cell line. The PS PC-Al chloride was as the reference compound since its fluorescence emission is in the red shift at the same region as the effective MA constituents. Pc-Al showed some PDT effect of 20% and 30% photodamage in both A549 and MCF-7, respectively with concentration of $29 \mu\text{g/mL}$ ($50 \mu\text{M}$) (Figure 7-A). Whereas, it exhibited higher phototoxicity with relatively low concentrations of $58 \mu\text{g/mL}$ ($100 \mu\text{M}$) (Figure 7-B). However, Pc-AL experienced also some aggregation at higher concentration of $86 \mu\text{g/mL}$ ($150 \mu\text{M}$), although, it still gave good phototoxic effects of 80% in A549 and 82% in MCF-7, (Figure 7-C). Likewise to BL effect, increasing RL exposure time by 5 min didn't show more remarkable effect on the above MA samples. The phototoxicity of all the three MA categories using RL irradiation was assessed similarly in LNCap and MDA MB-435. The phototoxic damage showed clear selective effect of some of MA samples for both LNCap and MDA MB-435 cell lines (Supporting Data, Figures S-3).

[Figure 7]

PDT Effect of MA constituents with dual light sources/ BL and RL

The effect of dual light irradiation (BL and RL) on MA constituents for both cellulase and lysozyme extracts was investigated to assess the possible existence of materials with dual photoactive functionalities. The 96-well plates with cells incubated with MA constituents

were first exposed to BL for 5 min followed by RL for 5 min, (Figure 8-A and -B). The efficacy of PDT using dual light sources of Category I and II samples determined in A549 and MCF-7 cell lines. The only sample that its phototoxic effect was increased in Category I was of MA-15 with photodamage values of ≈ 90 and ≈ 87 % in A549 and MCF-7 upon dual light activation, respectively. Whereas, MA-09 and -17 performed better with single BL light as compared to dual light exposure. Interestingly, the samples in Category II (MA-02, -08, -10, -16, -18, and -20) demonstrated significant increase to their phototoxic efficacy with both BL and RL irradiation. They all have up to 95 % phototoxic damage to both cell lines. Pc-A1 with concentration of 86 $\mu\text{g}/\text{mL}$ (150 μM) also increased its efficacy slightly in MCF-7 only to $\approx 90\%$, considering it required the RL for its activation.

[Figure 8]

Concentration dependence effects of MA on the cell's viability profile and the phototoxicity IC_{50} values

The concentration dependence of MA samples on the magnitude of the phototoxicity after activation with BL or RL were investigated in A549 and MCF-7 cancer cell lines. Several experimental optimizations were carried out and a range of MA concentrations were chosen for the samples that displayed PDT efficacy in order to calculate the values of 50 % cell death (IC_{50}) (presented in Table 2).

[Table 2]

The concentration range was between 200-1000 $\mu\text{g}/\text{ml}$ for Category I (MA-03, -07, -09, -15, and -17) and irradiated with BL, Category II (MA-02, -10, -16, -18, and -20), irradiated with RL after several experimental optimizations. The concentration range for Category III (MA-25 to MA-31) was between 20-100 $\mu\text{g}/\text{mL}$, owing to their higher effect. Pc-A1 was also used with Category III as reference compound with 5 concentrations between 20 to 100 $\mu\text{g}/\text{ml}$,

which was irradiated with RL too. The phototoxicity profile of all the above MA samples conferred positive correlation upon the concentration increase (Supporting Data S-4). The values of IC_{50} of Category I was between ≈ 309 to ≈ 700 $\mu\text{g/mL}$ for A549 and ≈ 314 to ≈ 986 $\mu\text{g/ml}$ for MCF7. The sample MA-09 exhibited the best value of the Category I of ≈ 309 $\mu\text{g/mL}$ in A549 and ≈ 314 $\mu\text{g/ml}$ in MCF-7. The values of IC_{50} for Category II were better than Category I, ranged between ≈ 130 to ≈ 542 $\mu\text{g/ml}$ in A549 and ≈ 179 to ≈ 429 $\mu\text{g/mL}$ in MCF-7. Category III samples exhibited the highest phototoxicity, ranging between ≈ 16 $\mu\text{g/mL}$ for MA-31 to ≈ 42 $\mu\text{g/mL}$ for MA-29 in A549, while the values of IC_{50} were between ≈ 7 $\mu\text{g/mL}$ for MA-31 to ≈ 50 $\mu\text{g/mL}$ for MA-29 in MCF-7 cells. The PDT efficiency of the Category III samples was in comparable range to the reference compound (Pc-Al), which has $IC_{50} \approx 24$ $\mu\text{g/mL}$ in A549 and ≈ 32 $\mu\text{g/mL}$ in MCF-7.

Dark/chemical cytotoxic effect of PSs

One of the characteristics of a good PS is being not harmful to the cells in the absence of light. Therefore, dark toxicity of MA constituents was investigated in A549 and MCF-7 cell lines without irradiating MA constituents Category I, II, and III (Fig 9, A, B, and C). In comparison to untreated control cells, MA constituents MA-01, -03, -05, -07, -11, -13, -19 and -21 caused 5-10 % toxicity in both cell lines under controlled absence of light conditions, whereas MA-09, -15, and -17 exhibited damaged 7% to 11% in A549 cells. They 2 to 4 % cytotoxicity to MCF-7 cells. The Category III displayed slightly more cytotoxic effects on both cell lines with lower concentrations of 100 $\mu\text{g/ml}$. The latter Category caused between 8% to 20% chemical toxicity in A549 and 3 to 20 % in MCF-7.

[Figure 9]

Discussion

In recent years, a great number of natural products, their derivatives, and many secondary metabolites, have been isolated from marine organisms. Among these agents are compounds with different activities as inhibitors of transformation of the normal cells into cancer cells, retraction of tumor cell growth and formation of micro-tumors, and induction of apoptosis [8].

Herein, we have investigated several MA constituents with light application and examined their photochemical potential on tumor cell lines as a part of a boarder investigation aimed to explore MA effects on viruses, and as antioxidant agents. Several samples isolated from different MA strains by three methods were evaluated in the most widespread cancer types (A549 and MCF-7) with PDT techniques. The details of extraction methods were previously published [27]. Our goal was to identify the most active extracts of semi-fractionated samples, allowing the isolate and characterize of their bioactive chemical components to take place in the next stage. Absorbance spectral analysis was the first tool to provide an insight to the components that might be present in the extracted samples.

In addition, the spectra of MA for certain samples in the three categories confirmed the existence of the three well-reported major classes of photosynthetic pigments in microalgae including fluorescent protein in variable percentages. The chlorophylls derivatives, carotenoids (carotenes and xanthophylls), and phycobilins were more pronounced in Category III. It is acknowledged that the fluorescence of the chlorophyll is quenching quickly. The characteristic features of the tetrapyrroles compounds, particularly chlorins as part of chlorophyll were shifted after removal of the coordinating magnesium. One of the key requirements of a good photosensitizer, is to have strong absorption with a high extinction coefficient in the red/near infrared region of the electromagnetic spectrum (600–850 nm) as these wavelengths allow deeper tissue penetration [30]. PS fluorescence emission has been considered a good marker to reflect local drug concentration or bioavailability for PDT

within the cell membrane [31]. It would account for indirect parameter (phototoxicity) to reflect the production of reactive oxygen species (ROS) and subsequently, the efficacy of their PSs [18, 23]. The strong fluorescence intensities for the majority of all the samples in the red shift indicated to the presence of chlorins as the major photosensitisation components. However, some samples emitted fluorescence below the red shift region where the groups such as coumarins, carotenoids, flavonoids could be also present [32]. It has been reported that the fluorescent protein family could be as blue fluorescent protein or yellow fluorescent protein to red fluorescent protein which considered as a source of excellent tools for live-cell imaging and auto-catalytically built in a host-independent process [33]. Measurement of the uptake of new photosensitive materials into cancer cells provides information on the (kinetics of) interaction and membrane transport characteristics of those materials. It enables a first rough estimation of their behavior to the light interval as a basis for identification of their constituents. The methodological approaches described here make use of the inherent fluorescence properties of the photosensitive constituents and allow for either absolute quantification of their active amount taken up by cells, i.e for estimation of time-dependent course of PS uptake. It was found out, the samples that conferred high fluorescence intensities, also exhibited high PDT efficacy in both cell lines using BL, RL, or dual (BL then RL) light sources with some specificity. The high efficacy of some samples was signifying their enrichment with PSs, not only the substances that might be emit their fluorescence at the red region of the light spectra, but also below that region. All the samples of Category III showed high efficacy against both cell lines (A459 and MCF-7) in variable degrees. On contrast, Pc-AI displayed much higher efficacy on the later cell line. Interestingly, by the level of the viable tumour cells, the prominent enhancement of PDT-Category I and II activated with dual BL followed by RL, in equal energy levels could be endorsed, regardless of their effects under BL or RL alone. This could be attributed to presence of different types

of constituents that existed at different region of light spectrum. Also, there are large naturally occurring molecules including proteins that feature two different light-sensing systems coexist in a single chromophore such as chromoprotein (phytochrome 3) [34]. It was reported that the N-terminal portion of phytochrome 3 contained the chromophore-binding domain of phytochrome (phytochromobilin), and the C-terminal half showed similarity to phototropin (pair of flavin derivatives), where both BL- and RL-dependent phototropic responses could occur [35]. Additionally, PDT effects by dual light activation could be owing to the presence of protein extracted from the light-driven outward sodium pump (KR2) such as channelrhodopsins found in the green alga *Chlamydomonas reinhardtii* (Chronos, and a red-sensitive channelrhodopsin named Chrimson) [35]. As a pair, these channelrhodopsins enabled independent multi-colour activation. MA constituents did not show great deal of toxicities without light exposure (in the dark) for the majority of the cells under investigation, in general; very few samples showed some cytotoxicity in certain cell lines. It was previously reported the inhibition effect of the ethanolic extracts of *Chaetoceros calcitrans* (MA) on cell growth of MCF-7 cells and MCF10A through the induction of apoptosis without cell cycle arrest. However, the components of the MA crude extracts would be variable and dependences on the methods of the extracts. The extracts could contain the photosensitisers that produce the reactive oxygen species (ROS) and in the same time the quenchers (antioxidants). The types, numbers, quantum yield of ROS, quantities of the photosensitive and the quencher's constituents in MA species, probably attributed to their variation responses to the BL light and RL exposure and their PDT efficacy [36].

The data presented in this study, clearly showed that MA constituents provide great source of potential photosensitizers and significantly caused photo-damage effects to various cancer cell lines. **To identify single chemical moieties in the semi-purified extracts from MA, chromatographic and spectroscopic analyses are required to determine the chemical**

composition. The next step of this work will be focused on the isolation of the potentially active novel PSs and to get a better understanding of the mechanisms and levels of phototoxic agents (ROS), selectivity, and intracellular localization within tumor cells. Among all tested strains, it was clearly seen that MA extracts from *Chlorella sp.* under all treatment methods (cellulose, lysozyme and ultrasonication) have shown good activity against both tumor cells (A549 and MCF-7), under all light conditions (blue, red and blue-red). Therefore, extracts from this strain appears to be the key candidates for the deeper investigation. In addition, extracts from the marine strains, namely *Nannochloropsis sp.* (MA-25) and *Tetraselmis sp.* (MA-26) could also be considered, which have shown good activity under red-light. The marine cultures have the advantage of growing in saline water, which reduces the freshwater load, needed by other strains.

Conclusions

Several MA products with antioxidant, anti-inflammatory and antitumor potentials which include tetrapyrroles, carotenoids, fatty acids, glycolipids, polysaccharides and proteins have not been explored in the field of PDT. Our study revealed the possibility of sourcing new molecules with photochemical properties that could be isolated and developed as PS agents from several MA species in the frame of PDT applications. The samples of Category I and II (especially, *Chorolla* and *M.C. sp.* samples) demonstrated variable efficacy with light and exerted their effect mostly with dual BL and RL. It is important to consider the possibility that more than one constituent may be involved in the observed synergetic biological activity, as the extracts are complex mixture of compounds. The samples of Category III extracted with ultra-sonication methods of *Scenedesmus*, *M.C. sp.*, and *Chlamydomonas* have great potential after RL activation and were the most effective photosensitiser. Whereas, the samples extracted with the same method from *Nannochloropsis*, *Tetraselmis*, and *A. braunii* pronounced significant specificities towards the tumor cell lines. In order to verify the chemical

composition of the semi-purified extracts from MA, chromatographic and spectroscopic analyses required to be carried out to identify single chemical moieties. Furthermore, it is essential to focus on isolation, purification, and categorization of the potentially active novel PSs. The development of new natural-PS contents of MA should allow more insights into the mechanisms of PDT, including the determination of the levels of the phototoxic agents (ROS), selectivity, and intracellular localization within tumor cells.

Acknowledgments

The authors would like to acknowledge the financial support provided by Zayed Center for Health Sciences (Fund# 31R019) and Chemstra Ltd, UK.

Conflicts of Interest

The authors declare no conflict of interest. The founding sponsors had no role in the design of the study; in the collection, analyses, or interpretation of data; in the writing of the manuscript, and in the decision to publish the results.

References

- [1] Lage H. An overview of cancer multidrug resistance: a still unsolved problem. *Cell Mol Life Sci.* 2008; 65(20): 3145-3167.
- [2] Perez-Tomas R. Multidrug resistance: retrospect and prospects in anti-cancer drug treatment. *Curr Med Chem.* 2006; 13(16): 1859-1876.
- [3] Lee DH, Iwanski GB, Thoennissen NH. Cucurbitacin: ancient compound shedding new light on cancer treatment. *Scientific World Journal.* 2010; 10: 413-418.
- [4] Amaro HM, Barros R, Guedes AC, Sousa-Pinto I, Malcataemail FX. Microalgal compounds modulate carcinogenesis in the gastrointestinal tract. *Trends Biotechnol.* 2013; 31(2): 92-98.
- [5] Talero E, García-Mauriño S, Ávila-Román J, Rodríguez-Luna A, Alcaide A, Motilva V. Bioactive Compounds Isolated from Microalgae in Chronic Inflammation and Cancer. *Mar Drugs.* 2015; 13(10): 6152-6209.
- [6] Delalat B, Sheppard VC, Rasi Ghaemi S, Rao S, Prestidge CA, McPhee G, Rogers ML, Donoghue JF, Pillay V, Johns TG, Kröger N, Voelcker NH. Targeted drug delivery using genetically engineered diatom biosilica. *Nat Commun.* 2015; 6: 8791.

- [7] Kilian O, Benemann CS, Niyogi KK, Vick B. High-efficiency homologous recombination in the oil-producing alga *Nannochloropsis* sp. *Proc Natl Acad Sci U S A*. 2011; 108(52): 21265-21269.
- [8] García-Vilas JA, Martínez-Poveda B, Quesada AR, Ángel Medina M. Aerophysinin-1, a Sponge-Derived Multi-Targeted Bioactive Marine Drug. *Mar Drugs*. 2015; 14(1): 1.
- [9] Markou G, Nerantzis E. Microalgae for high-value compounds and biofuels production: a review with focus on cultivation under stress conditions. *Biotechnol Adv*. 2013; 31(8): 1532-1542.
- [10] Nobrea BP, Villalobosb F, Barragánb BE, Oliveiraa AC, Batistaa AP, Marquesa PASS, Mendesa RL, Sovovád H, Palavrac AF, Gouveiaa L. A biorefinery from *Nannochloropsis* sp. microalga--extraction of oils and pigments. Production of biohydrogen from the leftover biomass. *Bioresour Technol*. 2013; 135: 128-136.
- [11] Begum H, Yusoff FM, Banerjee S, Khatoon H, Shariff M. Availability and Utilization of Pigments from Microalgae. *Crit Rev Food Sci Nutr*. 2015; 56(13): 2209-2222.
- [12] Costa LS, Fidelis GP, Cordeiro SL, Oliveira RM, Sabry DA, Câmara RBG, Nobre LTDB, Costa MSSP, Almeida-Lima J, Farias EHC, Leite EL, Rocha HAO. Biological activities of sulfated polysaccharides from tropical seaweeds. *Biomed Pharmacother*. 2010; 64(1): 21-28.
- [13] Wijesekara I, Pangestuti R, Kim S-K. Biological activities and potential health benefits of sulfated polysaccharides derived from marine algae. *Carbohydrate Polymers*. 2011; 84(1): 14-21.
- [14] Moussavou G, Kwak DH, Obiang-Obonou BW, Maranguy CAO, Dinzouna-Boutamba SD, Lee DH, Pissibanganga OGM, Ko K, Seo JI, Choo YK. Anticancer effects of different seaweeds on human colon and breast cancers. *Mar Drugs*. 2014; 12(9): 4898-4911.
- [15] Zandi K, Tajbakhsh S, Nabipour I, Rastian Z, Yousefi F, Sharafian S, Sartavi K. In vitro antitumor activity of *Gracilaria corticata* (a red alga) against Jurkat and molt-4 human cancer cell lines. *African Journal of Biotechnology*. 2010; 9(40): 6787-6790.
- [16] Stepanenko OV, Verkhusha VV, Kuznetsova IM, Uversky VN, Turoverov KK. Fluorescent proteins as biomarkers and biosensors: throwing color lights on molecular and cellular processes. *Curr Protein Pept Sci*. 2008; 9(4):338-69.
- [17] Bulina ME, Chudakov DM, Britanova OV, Yanushevich YG, Staroverov DB, Chepurnykh TV, Merzlyak EM, Shkrob MA, Lukyanov S, Lukyanov KA. A genetically encoded photosensitizer. *Nat Biotechnol*. 2006; 24:95-99
- [18] Mallidi S, Spring BQ, Chang S, Vakoc B, Hasan T. Optical Imaging, Photodynamic Therapy and Optically Triggered Combination Treatments. *Cancer J*. 2015; 21(3): 194-205.
- [19] Griffioen AW, Weiss A, Berndsen RH, Abdul UK, te Winkel MT, Nowak-Sliwinska P. The emerging quest for the optimal angiostatic combination therapy. *Biochem Soc Trans*. 2014; 42(6): 1608-1615.
- [20] Saviano S, Leon PE, Mangogna A, Tognetto D. Combined therapy (intravitreal bevacizumab plus verteporfin photodynamic therapy) versus intravitreal bevacizumab monotherapy for choroidal neovascularization due to age-related macular degeneration: a 1-year follow-up study. *Digit J Ophthalmol*. 2016; 30,22(2): 46-53.

- [21] Oniszczyk A, Wojtunik-Kulesza KA, Oniszczyk T, Kasprzak K. The potential of photodynamic therapy (PDT)—Experimental investigations and clinical use. *Biomed Pharmacother.* 2016; 83: 919-927.
- [22] Kereiakes DJ, Szyniszewski AM, Wahr D, Herrmann HC, Simon DI, Rogers C, Kramer P, Shear W, Yeung AC, Shunk KA, Chou TM, Popma J, Fitzgerald P, Carroll TE, Forer D, Adelman DC. Phase I drug and light dose-escalation trial of motexafin lutetium and far red light activation (phototherapy) in subjects with coronary artery disease undergoing percutaneous coronary intervention and stent deployment: procedural and long-term results. *Circulation.* 2003; 108(11): 1310-1316.
- [23] Agostinis P, Berg K, Cengel KA, Foster TH, Girotti AW, Gollnick SO, Hahn SM, Hamblin MR, Juzeniene A, Kessel D, Korbelik M, Moan J, Mroz P, Nowis D, Piette J, Wilson BC, Golab J. Photodynamic therapy of cancer: an update. *CA Cancer J Clin.* 2011; 61(4): 250-281.
- [24] Portale G, Hagen JA, Peters JH, Chan LS, DeMeester SR, Gandamihardja TA, DeMeester TR. Modern 5-year survival of resectable esophageal adenocarcinoma: single institution experience with 263 patients. *J Am Coll Surg.* 2006; 202(4): 588-596.
- [25] Muller PJ, Wilson BC. Photodynamic therapy of brain tumors--a work in progress. *Lasers Surg Med.* 2006; 38(5): 384-389.
- [26] Johansson A, Palte G, Schnell O, Tonn JC, Herms J, Stepp H. 5-Aminolevulinic acid-induced protoporphyrin IX levels in tissue of human malignant brain tumors. *Photochem Photobiol.* 2010; 86(6): 1373-1378.
- [27] Al-Zuhair S, Salaman S, Hisaindee S, Al Darmaki N, Battah S, Svistunenko D, Reeder B, Stanway G, Chaudhary A. Enzymatic pre-treatment of microalgae cells for enhanced extraction of proteins. *Eng. Life Sci.* 2017; 17: 175–185.
- [28] Zhang A, Wan L, Wu C, Fang Y, Han G, Li H, Zhang Z, Wang H. Simultaneous determination of 14 phenolic compounds in grape canes by HPLC-DAD-UV using wavelength switching detection. *Molecules.* 2013; 18(11): 14241-14257.
- [29] Amat, A, Clementi, C De Angelis, F Sgamellotti, A, and Fantacci. S. Absorption and Emission of the Apigenin and Luteolin Flavonoids: A TDDFT Investigation. *J. Phys. Chem. A.* 2009, 113: 15118–15126.
- [30] Allison RR; Moghissi K. Photodynamic Therapy (PDT): PDT Mechanisms. *Clinical Endoscopy.* 2013; 46(1): 24-29.
- [31] Lagorio MG, Cordon GB, Iriel A. Reviewing the relevance of fluorescence in biological systems. *Photochem Photobiol Sci.* 2015; 14(9): 1538-1559.
- [32] Schwartz SH, Qin X, Loewen MC. The biochemical characterization of two carotenoid cleavage enzymes from *Arabidopsis* indicates that a carotenoid-derived compound inhibits lateral branching. *J Biol Chem.* 2004; 279(45): 46940-46945.
- [33] Palma M. Cardenas-Jiron GI, Menendez Rodriguez MI. Effect of chlorin structure on theoretical electronic absorption spectra and on the energy released by porphyrin-based photosensitizers. *J Phys Chem A.* 2008; 112(51): 13574-1383
- [34] Kawai H, Kanegae T, Christensen S, Kiyosue T, Sato Y, Imaizumi T, Kadota A, Wada M. Responses of ferns to red light are mediated by an unconventional photoreceptor. *Nature.* 2003; 421(6920): 287-290.

- [35] Panzarini E, Inguscio V, Dini L. Overview of Cell Death Mechanisms Induced by Rose Bengal Acetate-Photodynamic Therapy. *International Journal of Photoenergy*. 2011; Article ID 713726, 11 pages.
- [36] Baudalet PH, Gagez AL, Bérard JB, Juin C, Bridiau N, Kaas R, Thiéry V, Cadoret JP, Picot L. Antiproliferative Activity of *Cyanophora paradoxa* Pigments in Melanoma, Breast and Lung Cancer Cells. *Mar. Drugs*. 2013; 11: 4390-4406

Tables Captions

Table 1. MA constituents (numbers assigned to samples of different extraction methods)

Table 2: IC₅₀ for A549 and MCF-7 cell lines treated with different MA samples

Figures Captions

Figure 1. MA Absorbance spectra of microalgae (A), (B), and (C) for the three categories. The spectra of each sample and the absorbance at 400 nm, were measured by diode array at room temperature

Figure 2. MA fluorescence spectra of microalgae (A), (B), and (C) for the three categories in A549. The spectra of the control cells (cells without MA) were deducted from each spectra of the photosensitizer. The cells with the incubated samples were excited at 400 nm. The cells were scanned and the emission spectra were recorded between 600 to 850 nm.

Figure 3. Fluorescence intensity profile of microalga samples in two cell lines (A549 and MCF-7). (A) MA constituents (Category I), (B) MA constituents (Category II). The cells with the incubated samples were excited at a wavelength of 400 nm and the fluorescence intensities were recorded at a wavelength of 670 nm. Error bars represent standard deviation and $0.001 < P < 0.05$

Figure 4. Fluorescence intensity profile of microalga samples in (A) A549 cells and (B) MCF-7 Cells (B) for MA constituents (Category III). Cells were incubated with a range of concentrations between 100-500 µg/mL for 24 h. The excitation wavelength was 400 nm and the fluorescence and emission intensities wavelength were 670 nm. Error bars represent standard deviation

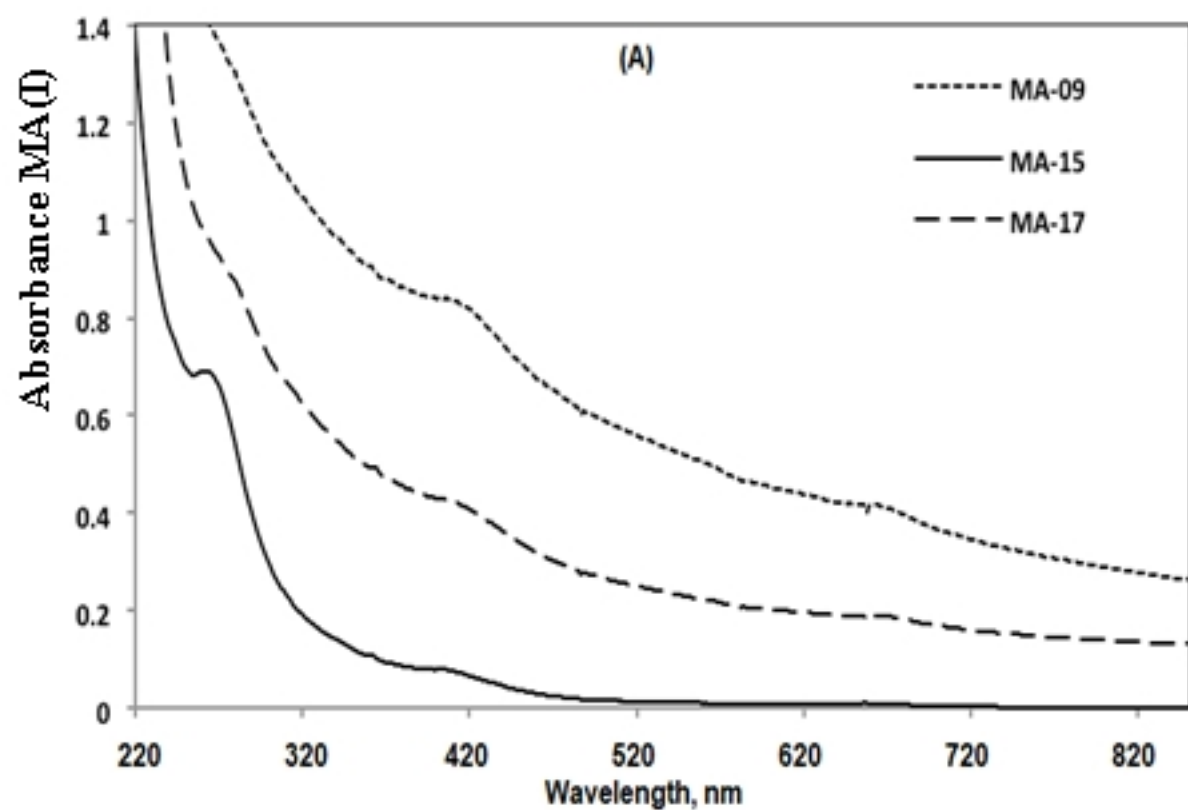
Figure 5. A549 cell line treated with MA constituents (Categories I and III) (Red). Gray DIC (differential interference contrast), Overlay (combined image of red and DIC). Scale bar 50 µm. Grey DIC (differential interference contrast), Overlay (combined image red and DIC). Scale bar 50 µm

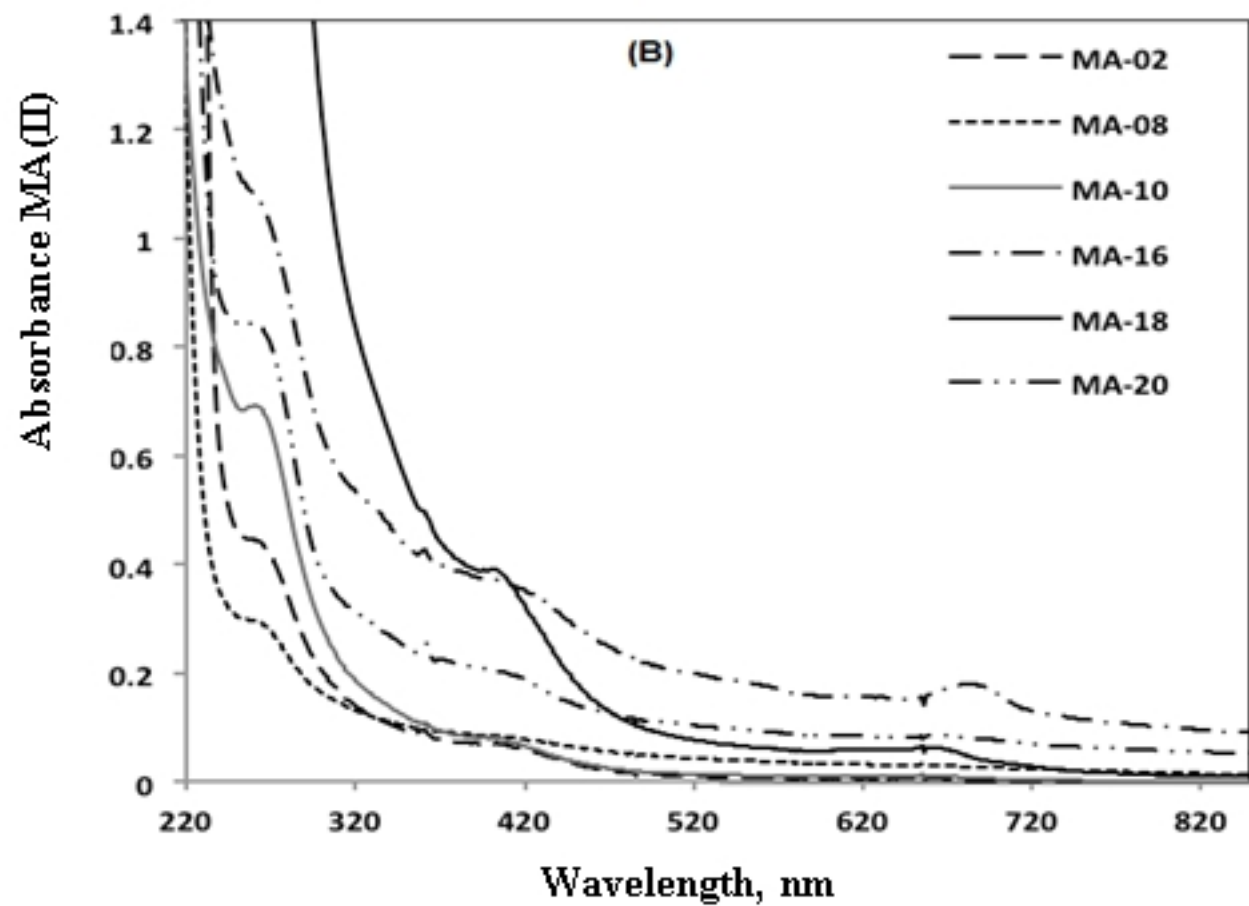
Figure 6. Comparison of PDT effect of MA constituents on A549 and MCF-7 viability with BL exposure for 10 min. Cells were incubated with 500 µg/mL of (A) MA constituents (Category I), and (B) MA constituents (Category II). Error bars represent the standard deviation of three wells and $0.005 < P < 0.05$

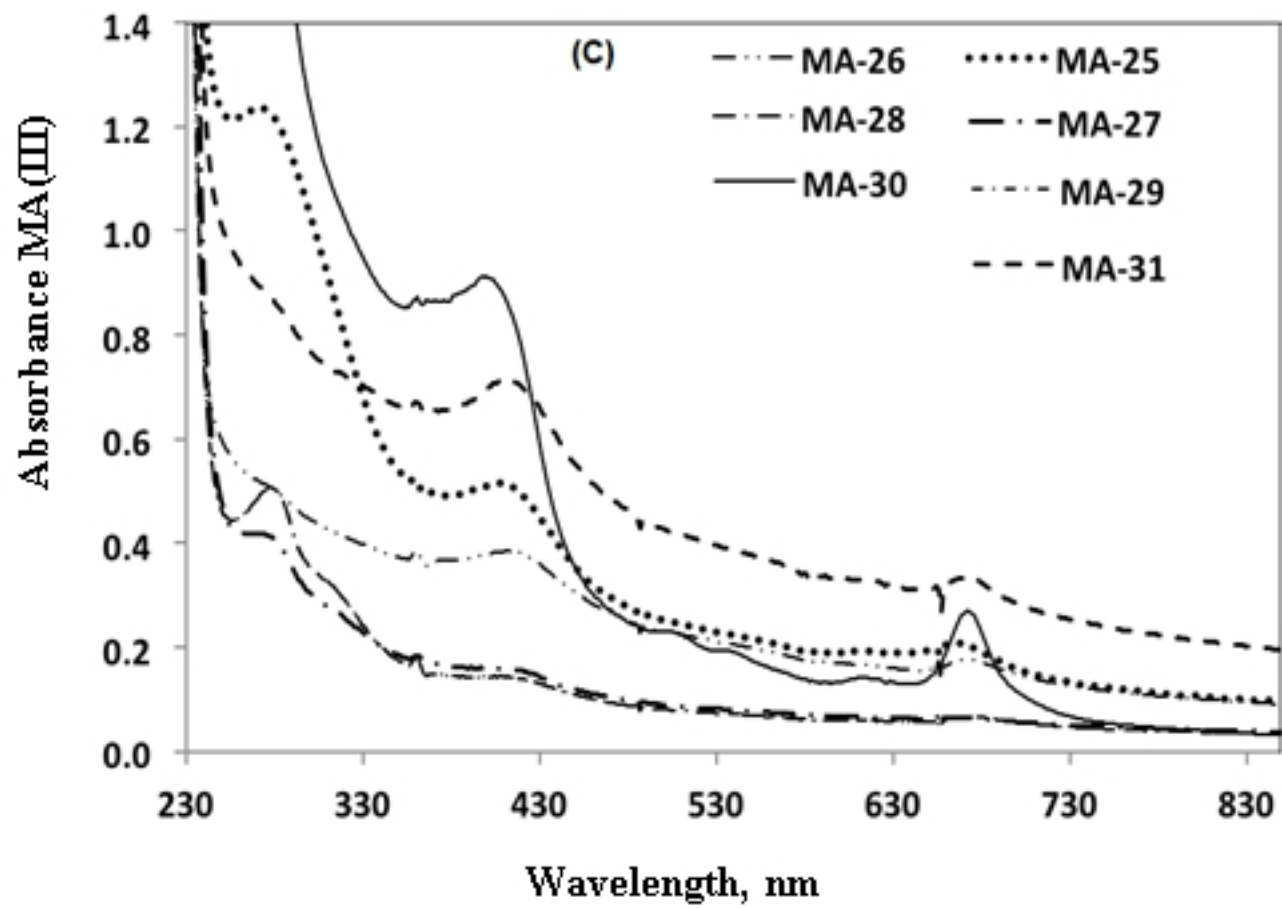
Figure 7. Comparison of PDT effect of MA constituents on the viability of A549 and MCF-7 with RL exposure for 5 min. Cells incubated with: (A) MA constituents (Category I) at a concentration of 500 µg/mL and Pc-Al at a concentration of 29 µg/mL (50 µM) as reference, (B) MA constituents (Category II) at a concentration of 500 µg/mL and Pc-Al at a concentration of 58 µg/mL (100 µM) as reference, and (C) MA constituents (Category III) at a concentration of 100 µg/mL and Pc-Al at a concentration of 86 µg/mL (150 µM) as reference. The control was untreated cells in each well plate. Error bars represent standard deviation, and $0.005 < P < 0.05$

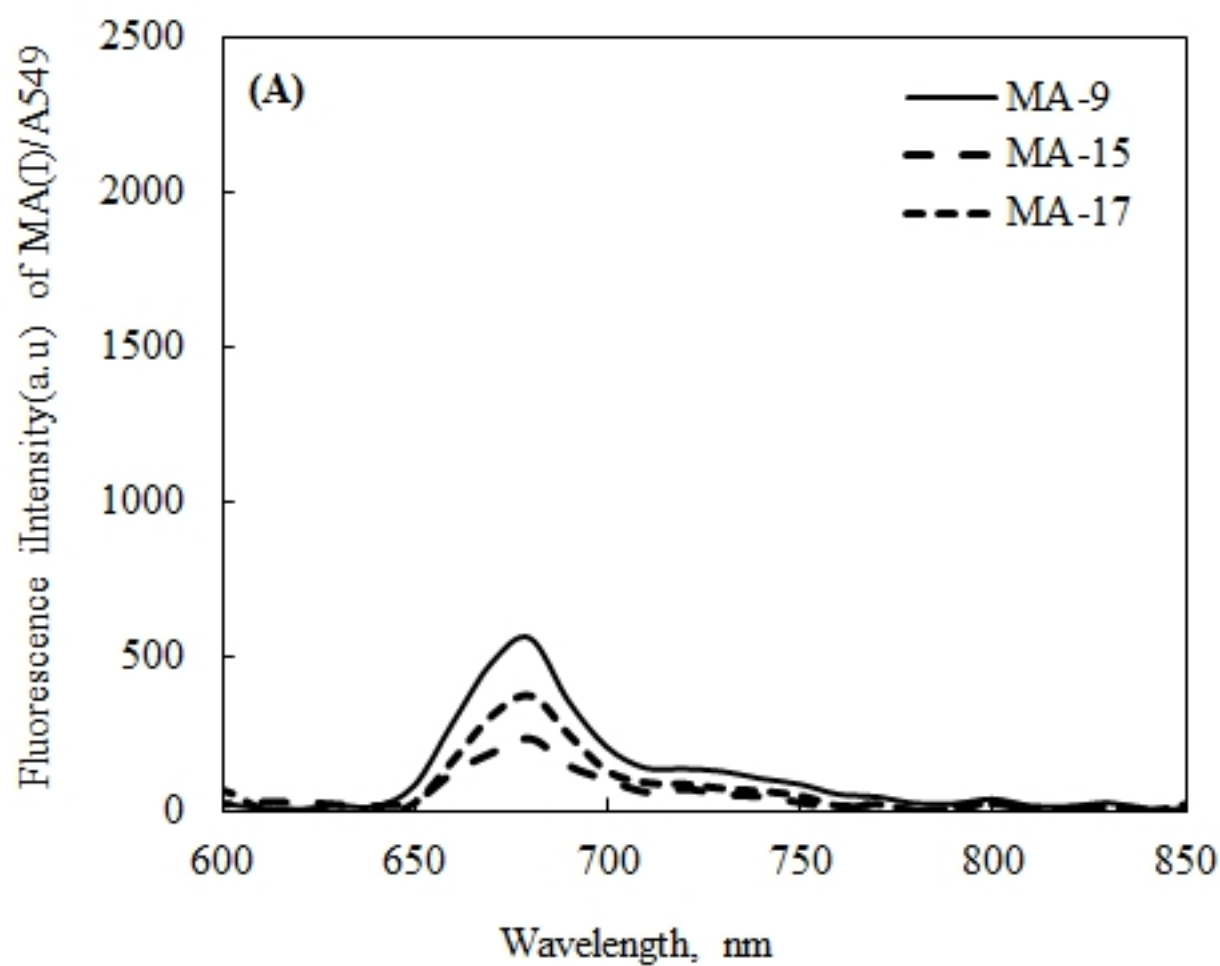
Figure 8. PDT effect of MA samples at a concentration of 500 µg/ml on A549 and MCF-7 irradiated with dual light sources (BL and RL) for 5 min each. (A) MA constituents (Category I), and (B) MA constituents (Category II). Pc-Al at a concentration of 86 µg/mL (150 µM) was used as a reference. Error bars represent standard deviation, and $0.005 < P < 0.05$

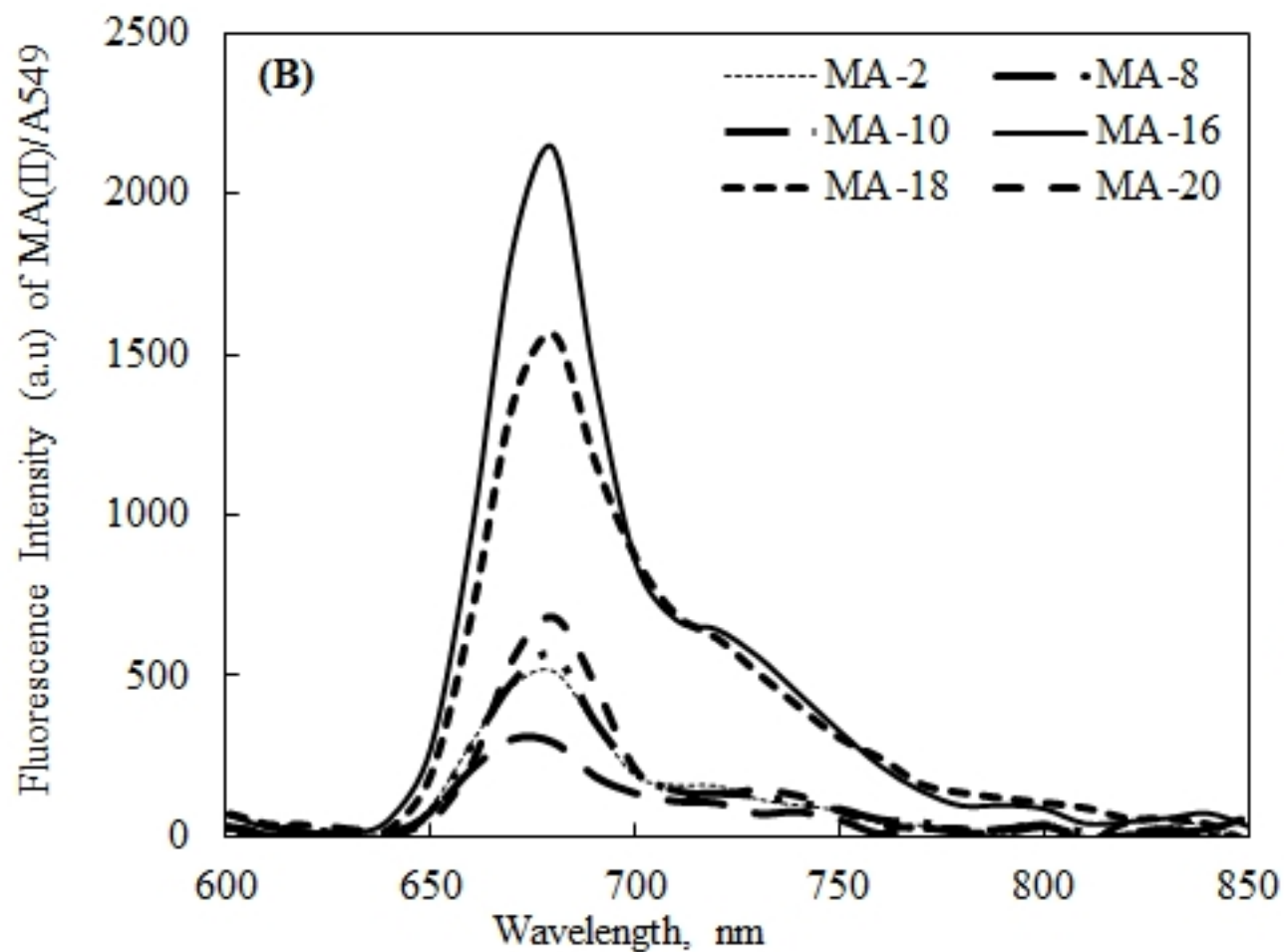
Figure 9. Dark cytotoxicity effect of MA samples on A549 and MCF-7 treated with 500 µg/mL MA constituents for 24 h. (A) Microalgae constituents (Category I), and (B) Microalgae constituents (Category II)

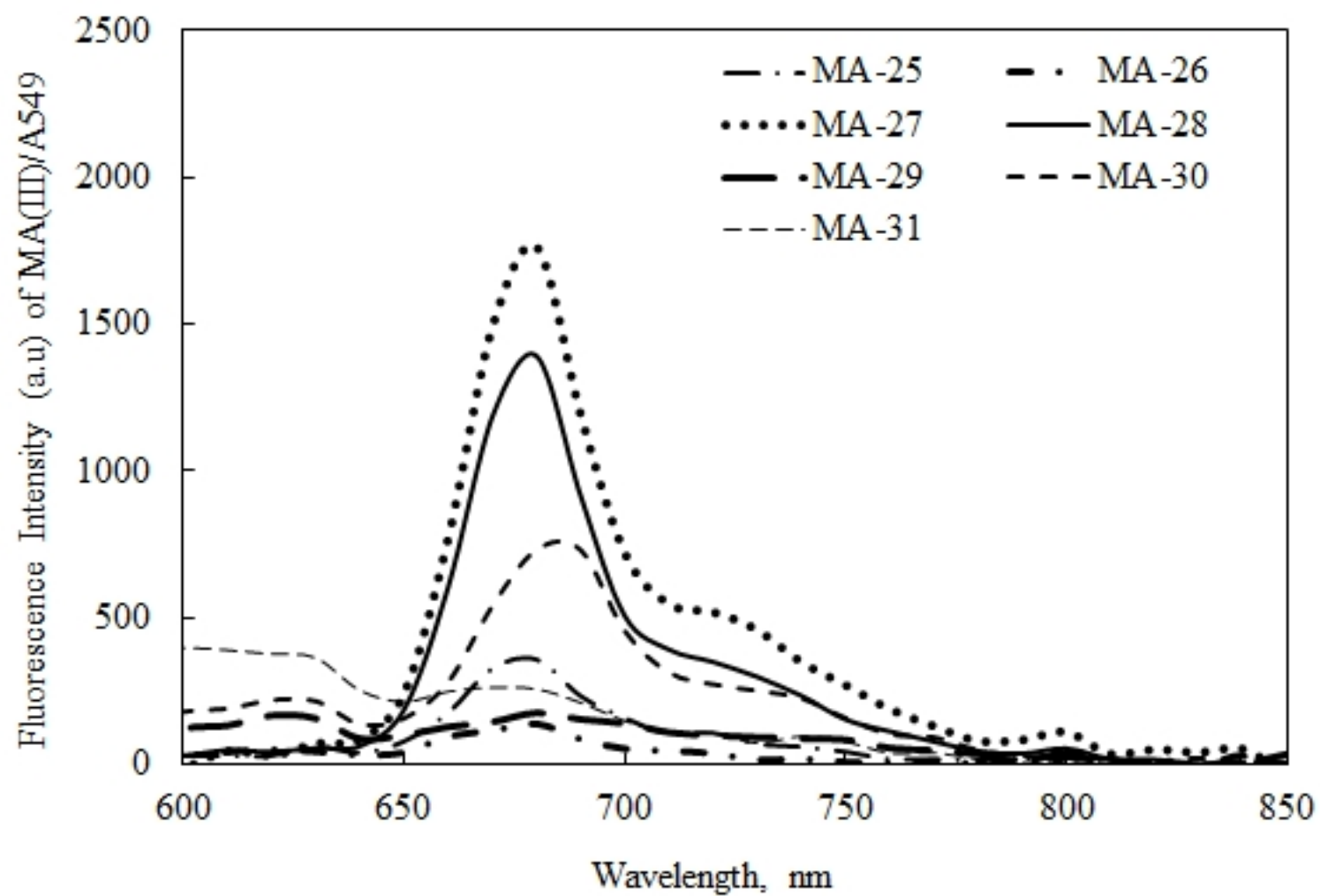


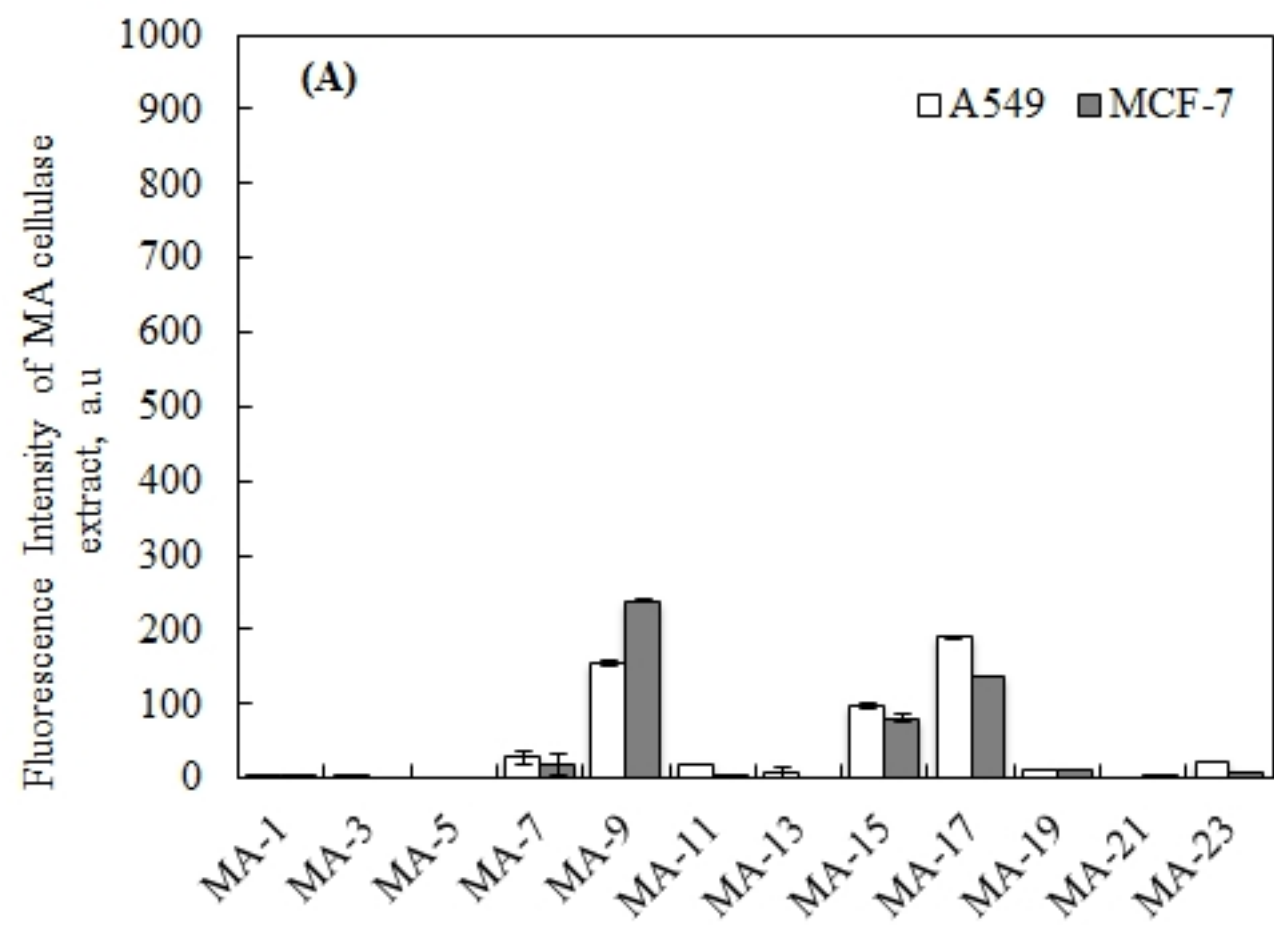


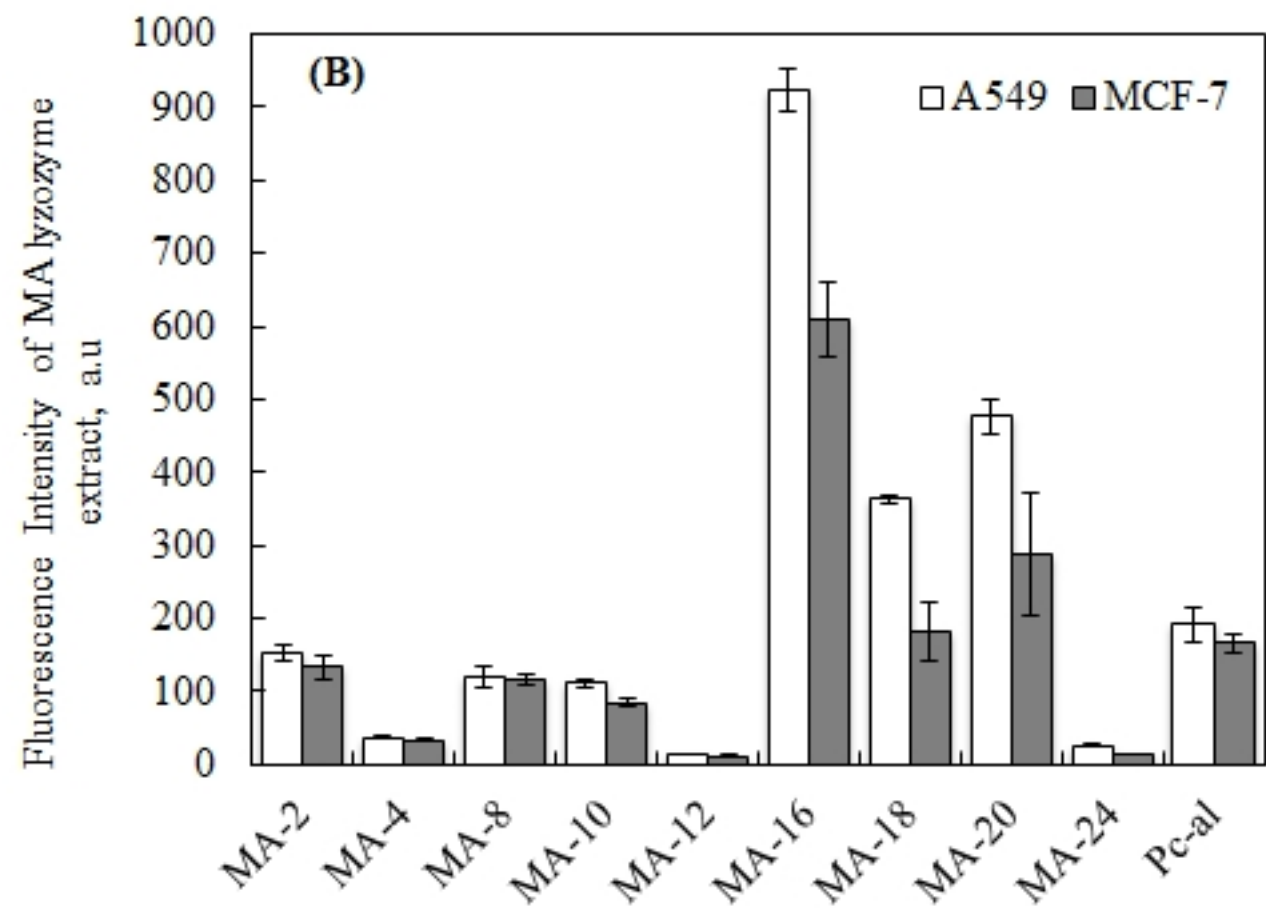


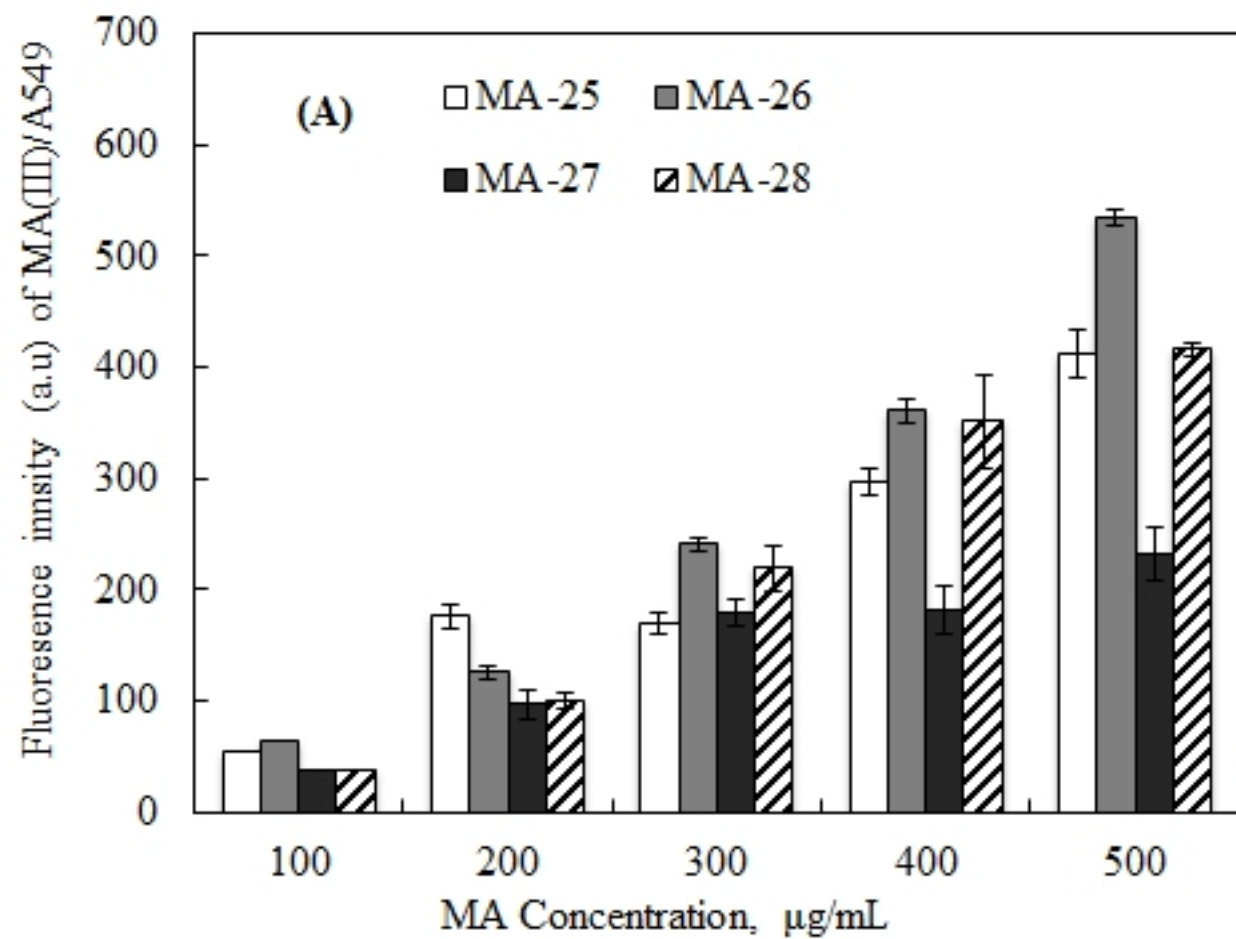


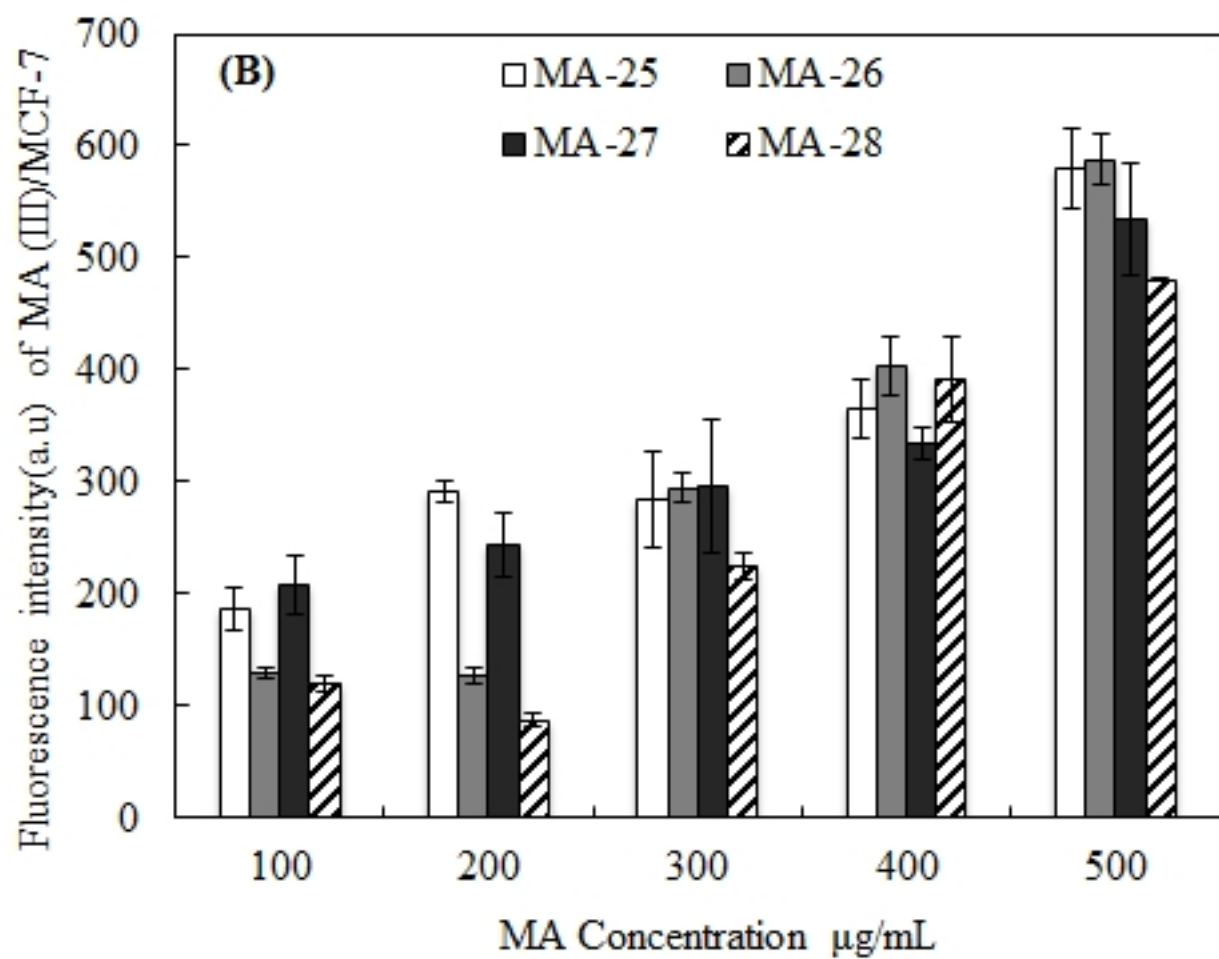


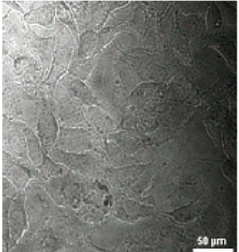
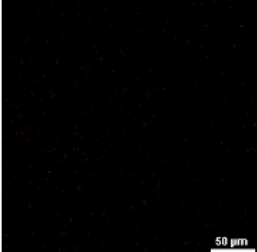
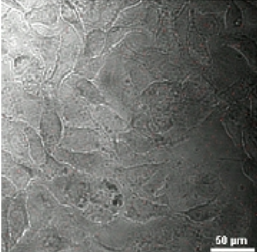
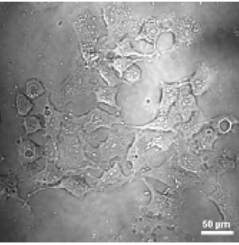
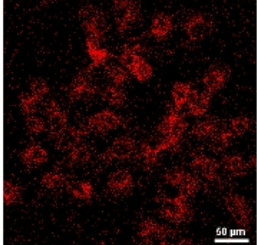
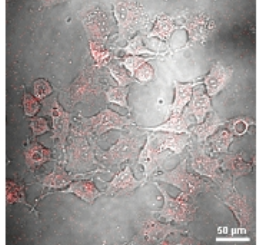
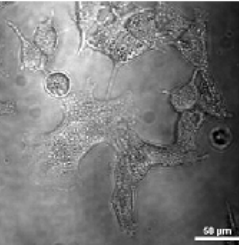
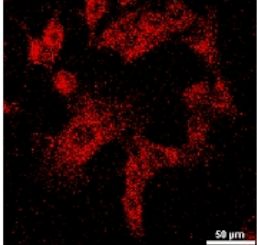
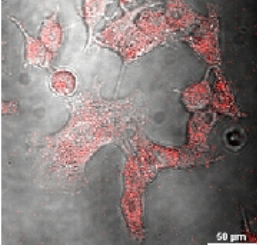
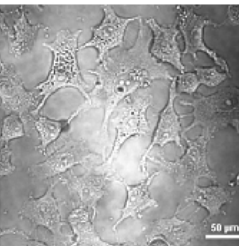
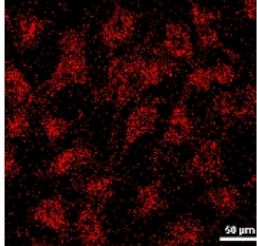
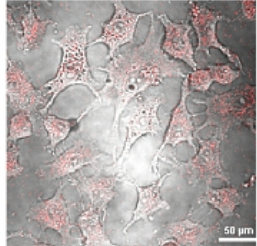
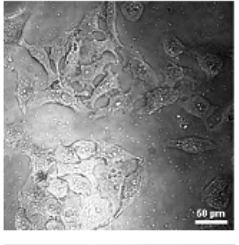
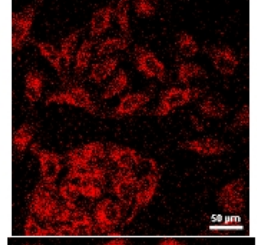
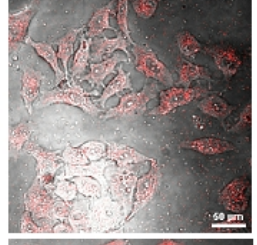
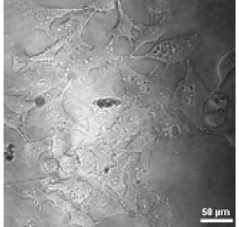
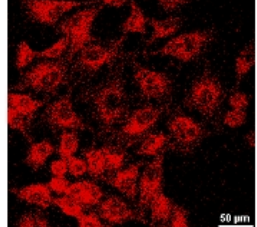
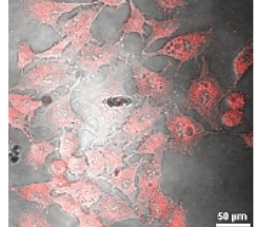


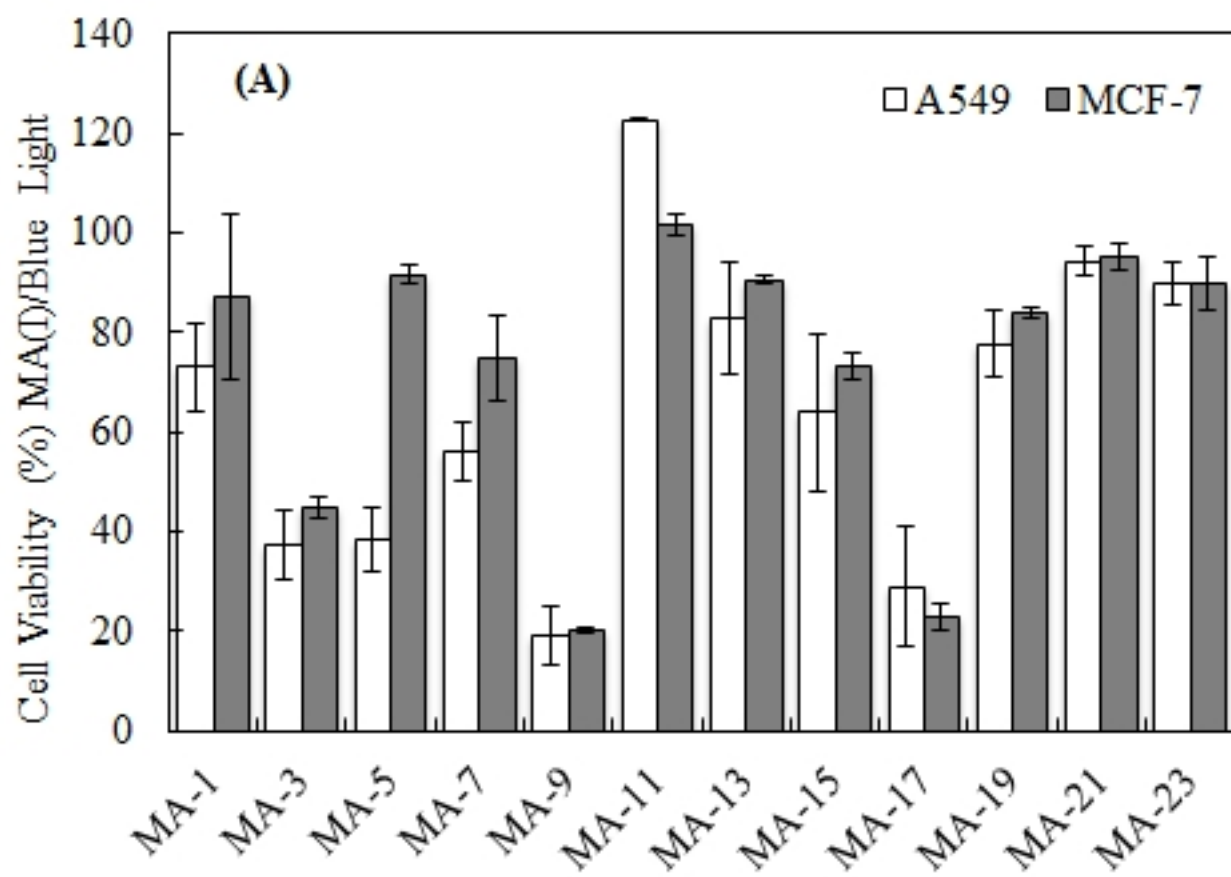


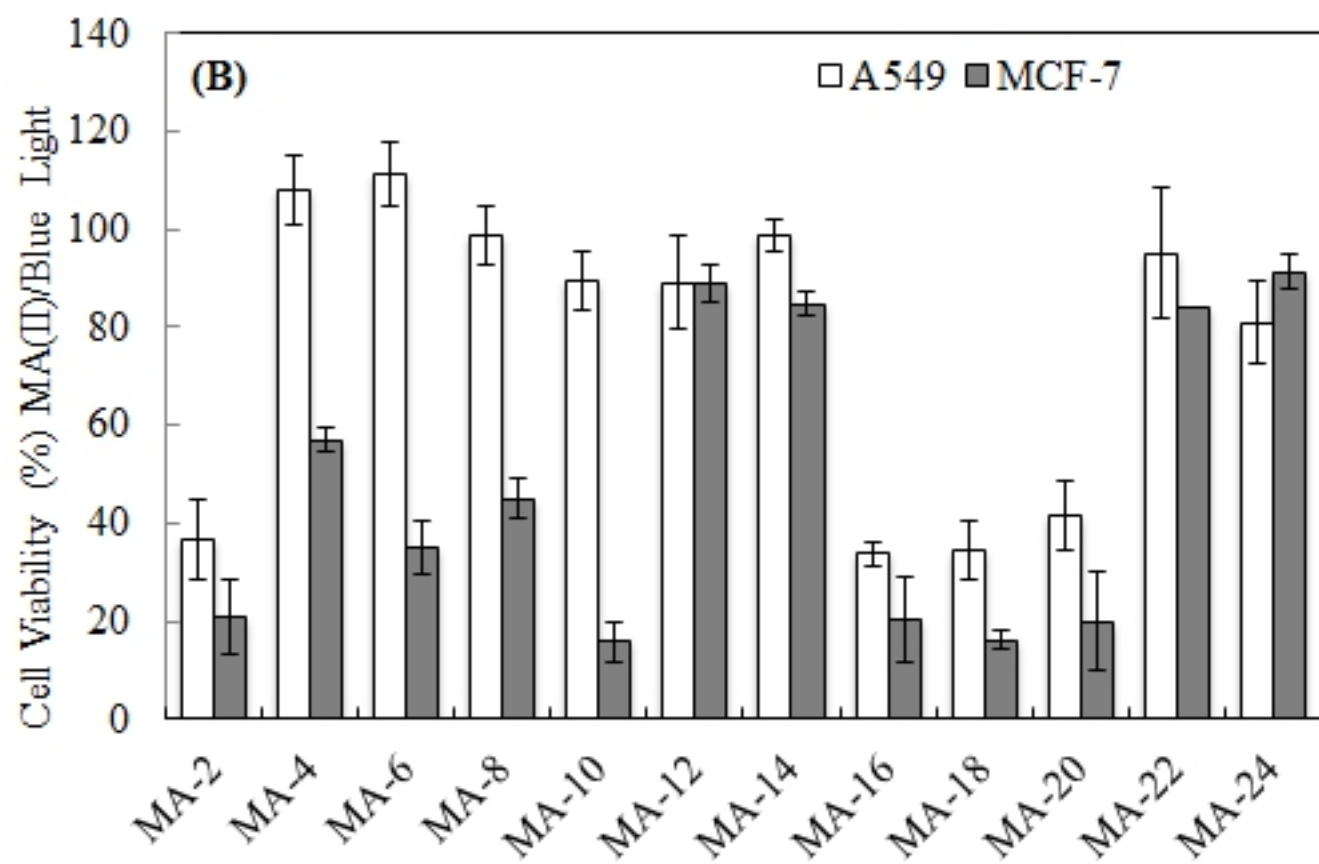


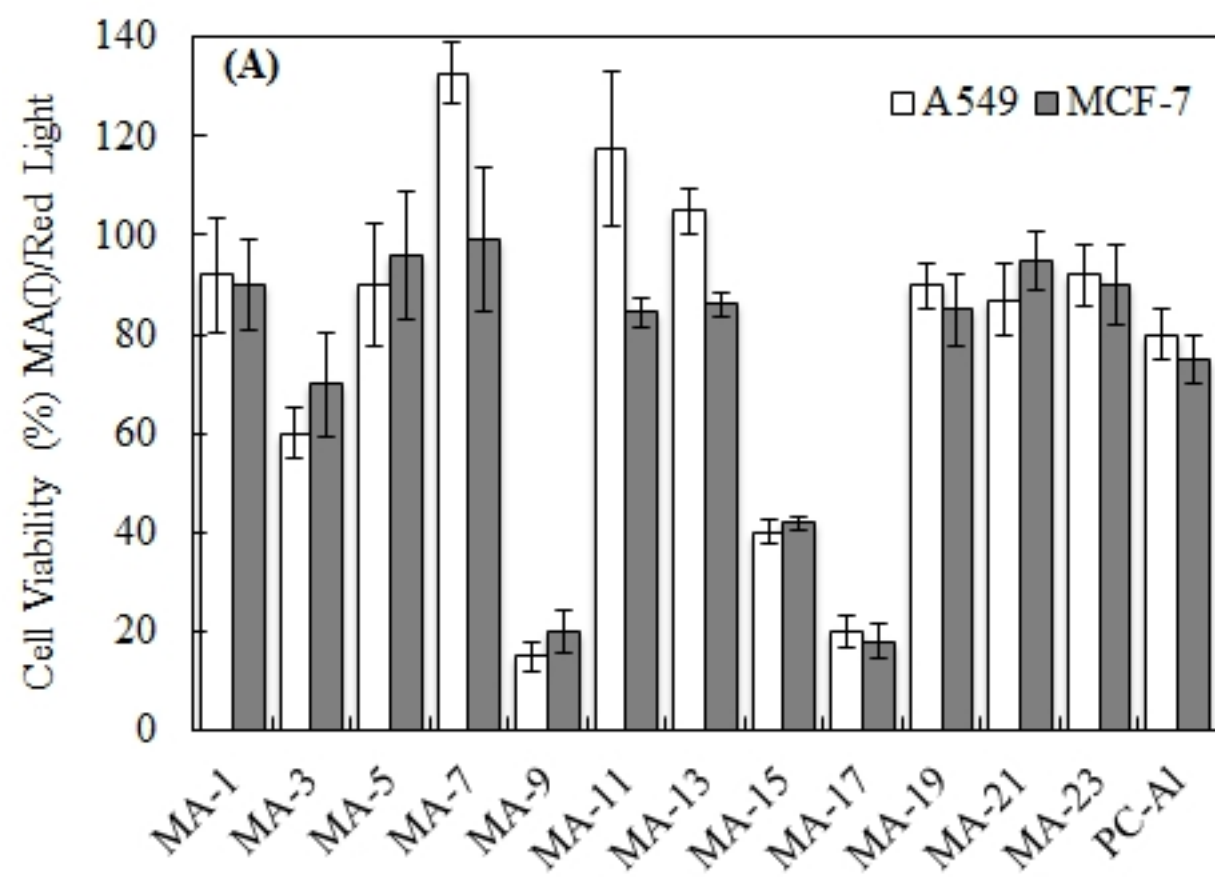


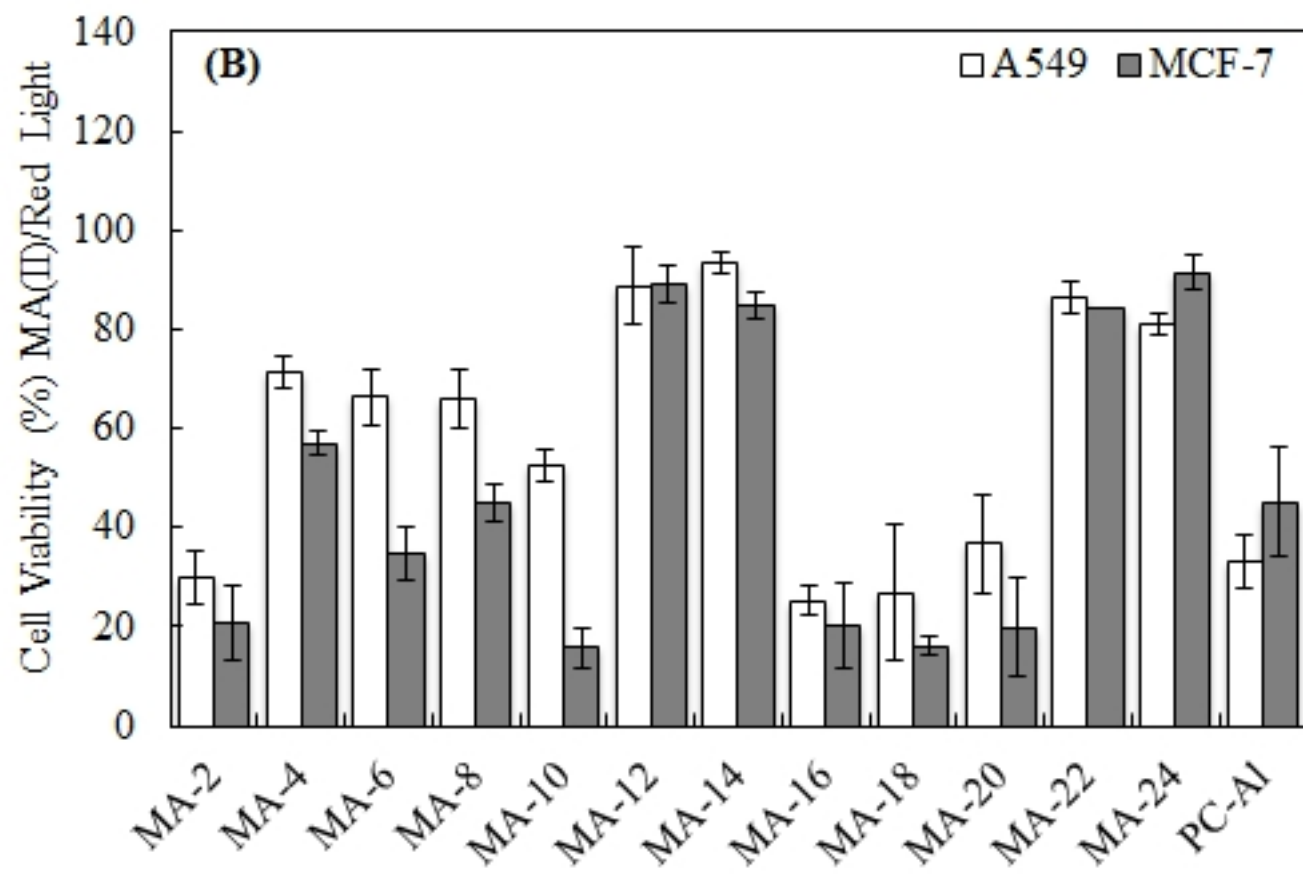


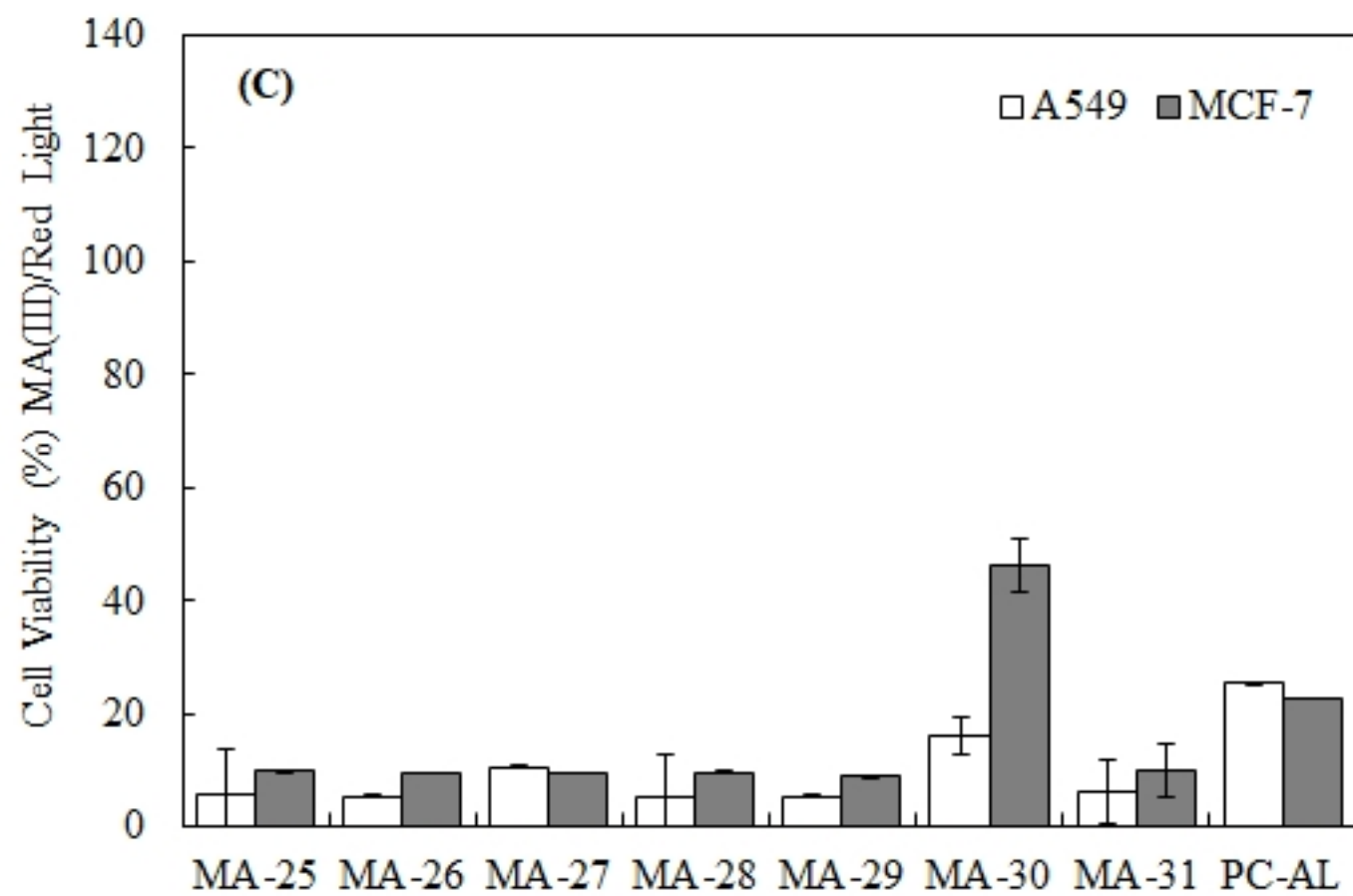
MA extract Sample	DIC (Grey)	Red (Emission at 700nm)	Overlay of DIC and Red
Control			
MA-02			
MA-16			
MA-18			
MA-30			
MA-31			

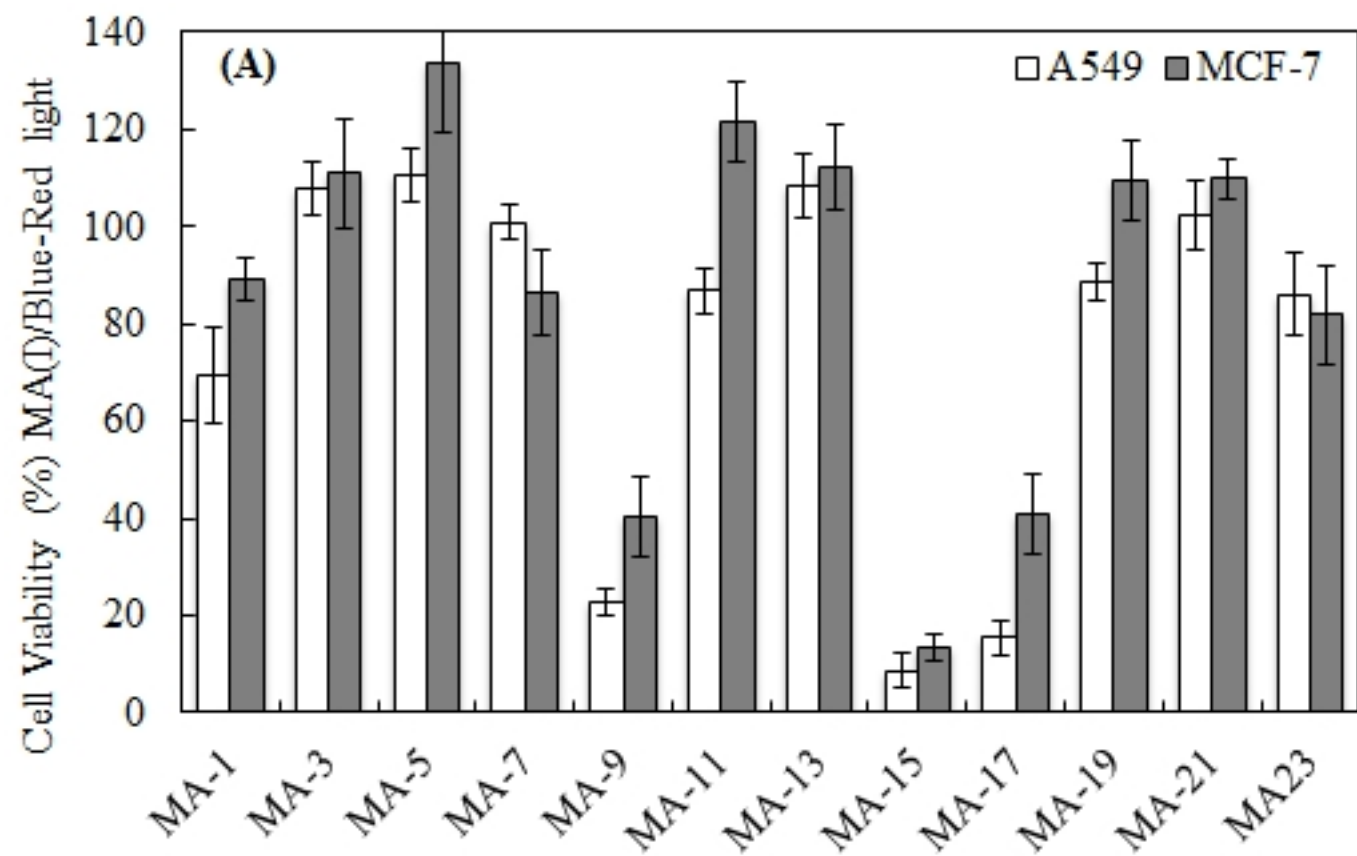


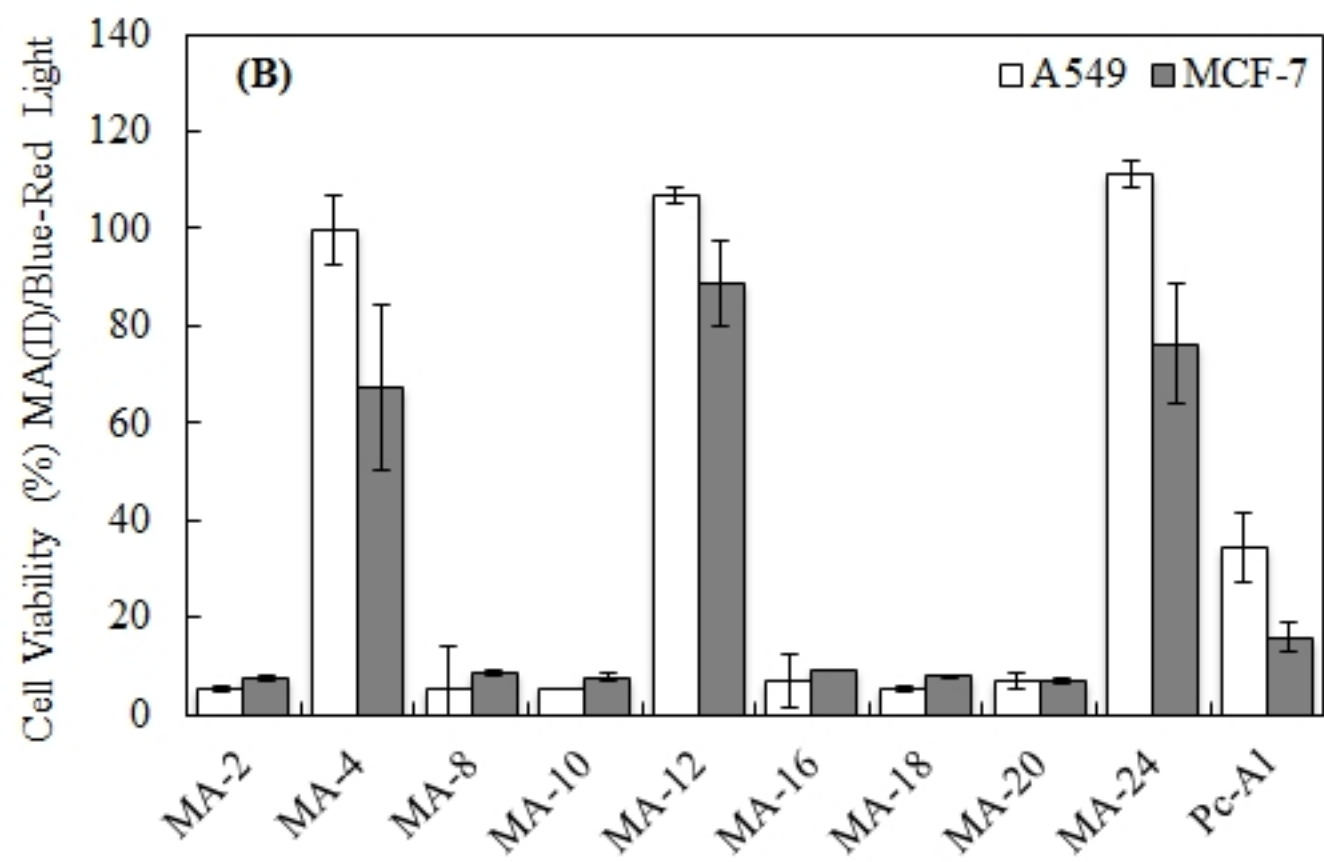


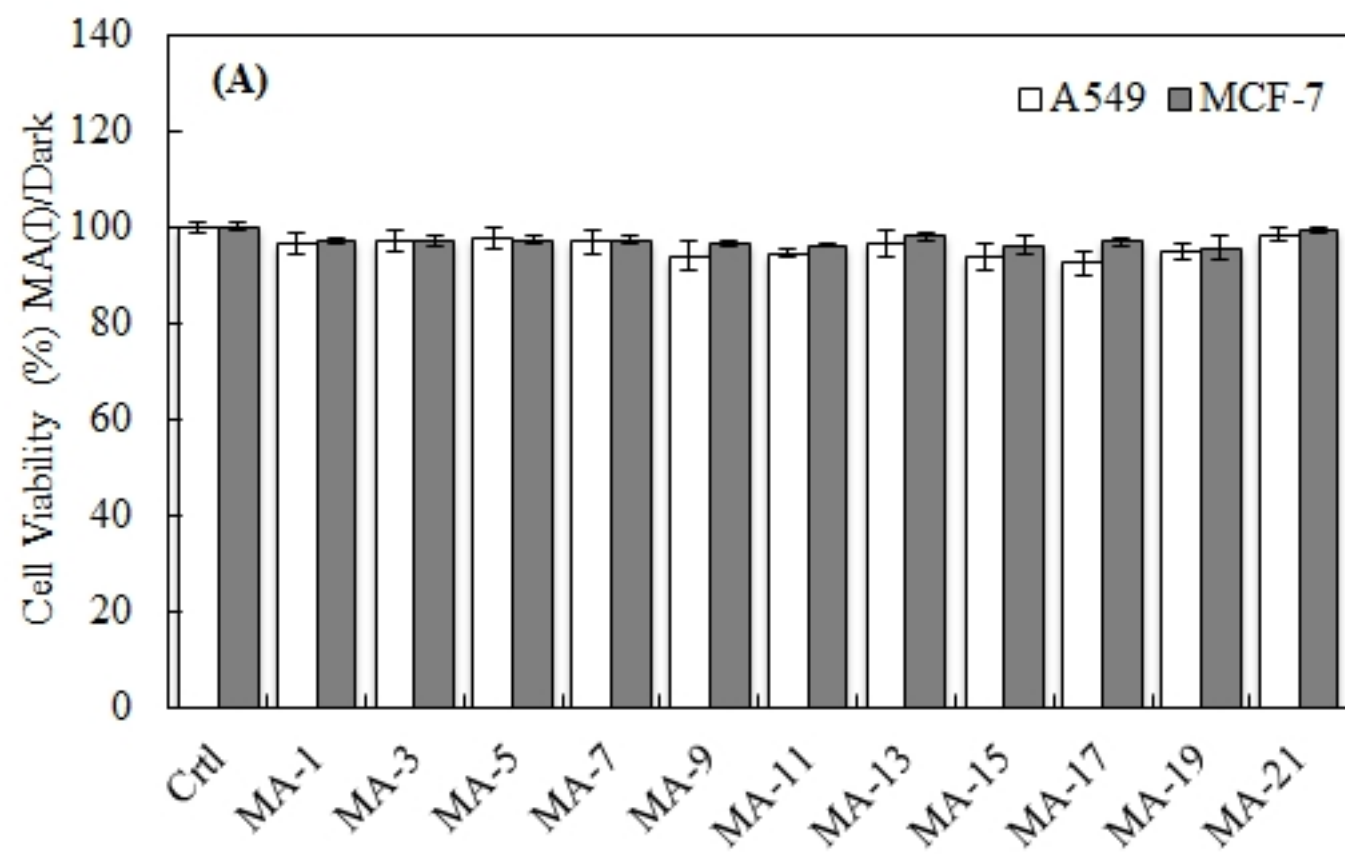












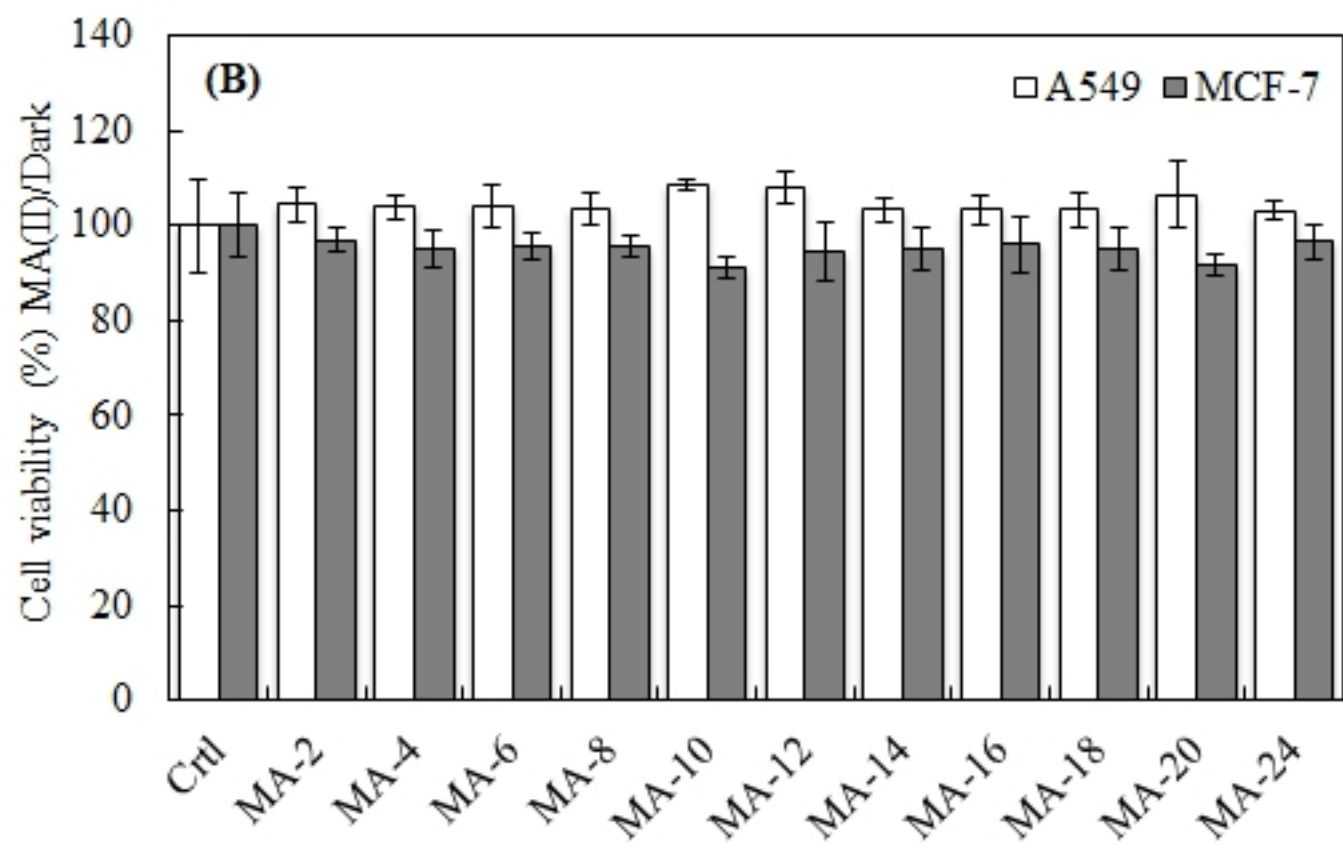


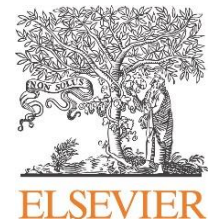
Table 2

Cat. I/BL	A549 μg/mL	MCF-7 μg/mL
MA-03	399.4 ± 6.9	453.7 ± 10.2
MA-07	569.5.2 ± 5.7	986.0 ± 8.7
MA-09	309.4 ± 6.1	313.7± 0.7
MA-15	695.4 ± 15.8	930.2 ± 2.6
MA-17	352.3 ± 12.1	325.1 ± 2.7

Cat. II/RL	A549 μg/mL	MCF-7 μg/mL
MA-02	501.3 ± 7.2	274.3 ± 4.1
MA-10	542.4 ± 6.2	178.7 ± 7.1
MA-16	130.4 ± 6.7	180.5 ± 1.4
MA-18	218.5 ± 4.9	180.9 ± 4.8
MA-20	214.5 ± 5.1	429.3 ± 5.3

Cat. III/RL	A459 μg/mL	MCF-7 μg/mL
MA-25	29.4 ± 3.7	28.5 ± 5.7
MA-26	19.7 ± 2.2	20.5 ± 6.3
MA-27	18.6 ± 2.3	7.5 ± 3.6
MA-28	23.0 ± 2.8	30.7 ± 5.4
MA-29	42.4 ± 4.7	50.1 ± 4.4
MA-30	17.4 ± 0.6	8.7 ± 4.2
MA-31	16.2 ± 1.8	7.3 ± 4.5
PC-AI	24.2± 6.0	31.9 ± 7.1

Author responsibilities, integrity, ethics



Article title :

Human and animal rights

The authors declare that the work described has been carried out in accordance with the [Declaration of Helsinki](#) of the World Medical Association revised in 2013 for experiments involving humans as well as in accordance with the EU Directive [2010/63/EU](#) for animal experiments.

Not applicable.

Informed consent and patient details

The authors declare that this report does not contain any [personal information](#) that could lead to the identification of the patient(s).

The authors declare that they obtained a written [informed consent](#) from the patients and/or volunteers included in the article. The authors also confirm that the personal details of the patients and/or volunteers have been removed.

Disclosure of interest

The authors declare that they have no known [competing financial](#) or [personal relationships](#) that could be viewed as influencing the work reported in this paper.

The authors declare the [following financial](#) or [personal relationships](#) that could be viewed as influencing the work reported in this paper:

Funding

This work did not receive any [grant](#) from funding agencies in the public, commercial, or not-for-profit sectors.

This work has been [supported](#) by:

Author contributions

All authors attest that they meet the current International Committee of Medical Journal Editors ([ICMJE](#)) criteria for Authorship.

Acknowledgements

Author Statement

This paper is a result of a collaborative work between UAE University, UAE, and Essex University, UK.

The role of each author is explained below:

Asma Jabeen (Research Assistant, School of Biological Sciences, Essex University) carried out all biological tests.

Brandon Reeder (Lecturer, School of Biological Sciences, Essex University) is an expert in oxidative damage of protein, haemoglobin, myoglobin, and antioxidants. Contribution of Dr. Reeder in this work was in the analysis of the biological results and the preparation of the manuscript.

Dimitri Svistunenko (Lecturer, School of Biological Sciences and Director of biomedical EPR facility, Essex University) is an expert in strength evaluation (ROS production) and protein oxidative damage after cancer and antioxidants treatments. Contribution of Dr. Svistunenko in this work was in the design of the biological experiments and the analysis of the results.

Soleiman Hisaindee (Associate Professor, Chemistry Department, UAE University) is an expert in Organic Chemistry. Contribution of Dr. Hisaindee in this work was in the analysis of the biological results and preparation of the manuscript

Salman Ashraf (Professor, Chemistry Department, UAE University) is an expert in Biochemistry. Contribution of Prof. Ashraf in this was in the protein extraction and analysis experiments. He also assisted in the analysis of the biological results and the preparation of the manuscript

Sulaiman Al-Zuhair (Professor, Chemical Engineering, UAE University) is a corresponding author of the paper. Contribution of Prof. Al-Zuhair in this work was in the microalgae cultivation and harvesting, cell disruption and protein extraction. In addition, he assisted in the analysis of the results and the preparation of the manuscript.

Sinan Battah (School of Biological Sciences, Essex University) is a corresponding author of the paper. Dr. Battah designed and supervised the biological tests. She also contributed in the analysis of the results and preparation of the manuscript.

Supporting Data

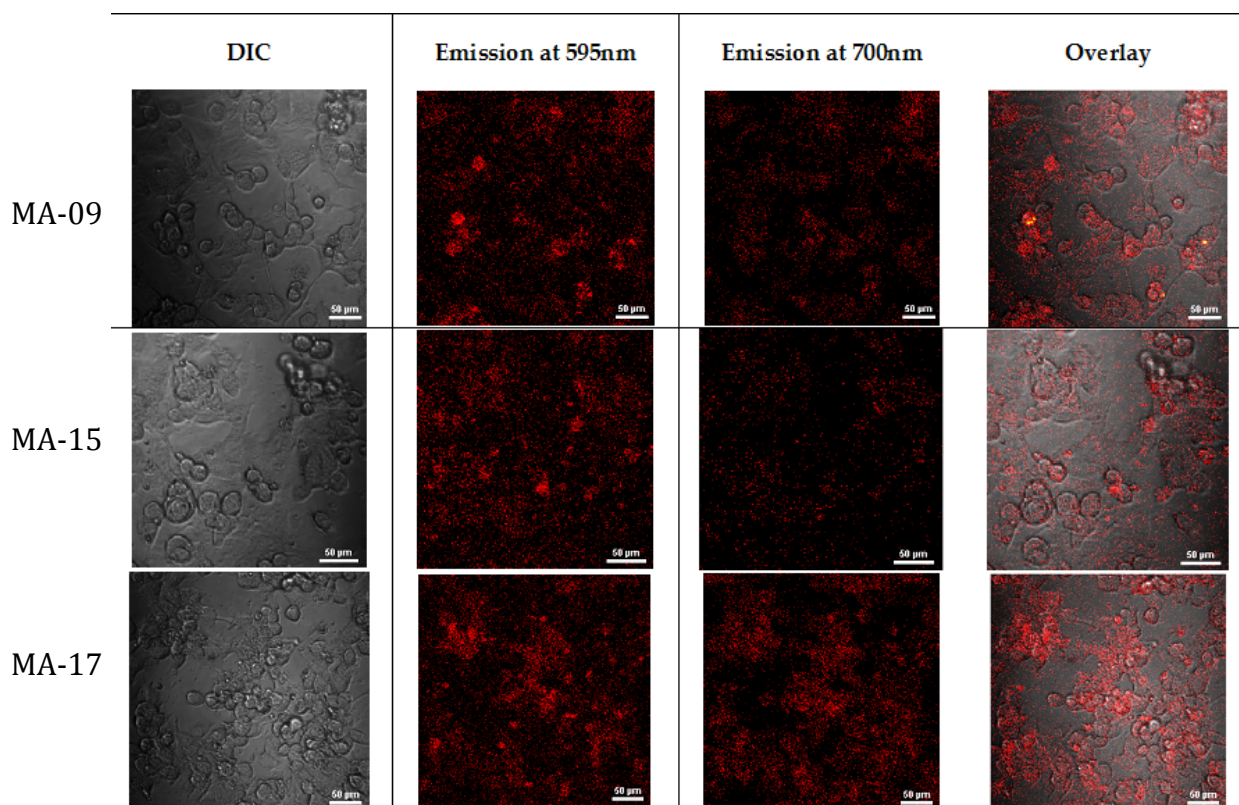


Figure S-1: LNCap cell line treated with MA constituents (Categories I) (Red). Gray DIC (differential interference contrast), Overlay (combined image of red and DIC). Scale bar 50 μm . Grey DIC (differential interference contrast), Overlay (combined image red and DIC). Scale bar 50 μm

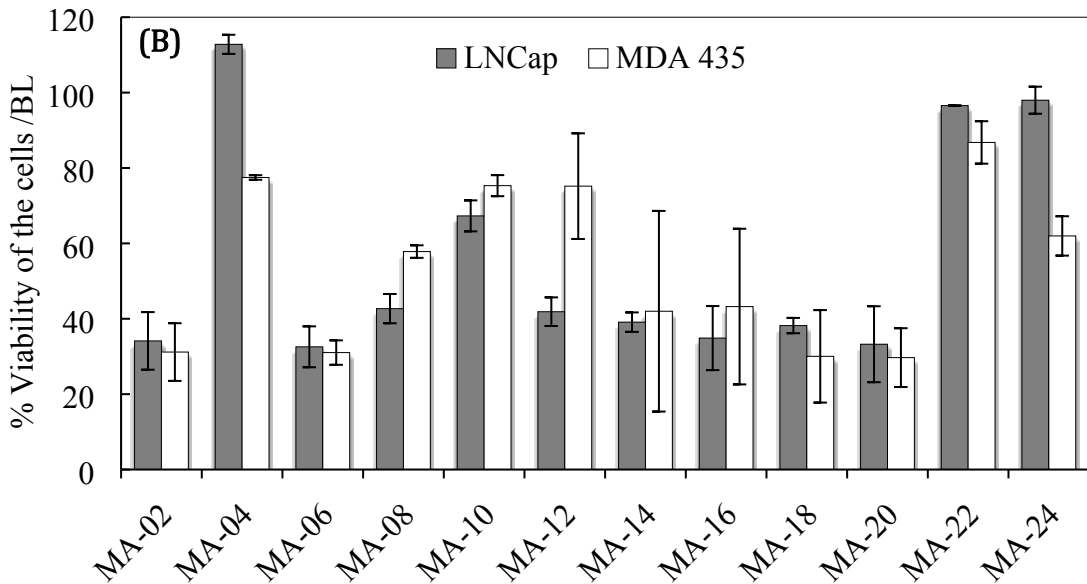
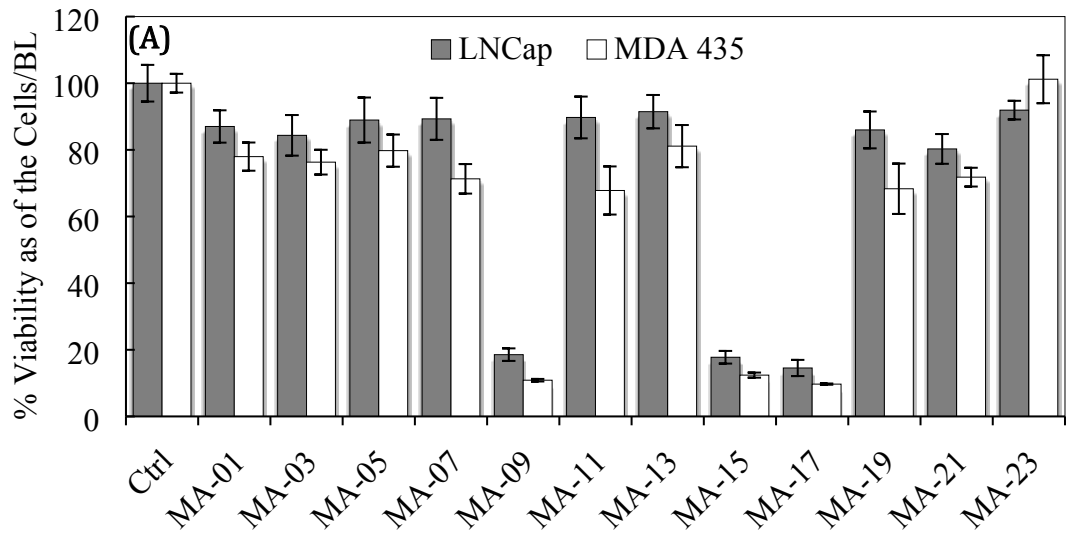


Figure 11

Figure S-2: Comparison of PDT effect of MA constituents on LNCap and MDA 435 viability with BL exposure. Cells were incubated with Category I and II. (500 $\mu\text{g}/\text{mL}$) and the plates were exposed to BL for 10 min. Error bars represent the standard deviation of three wells and $0.005 < P < 0.05$

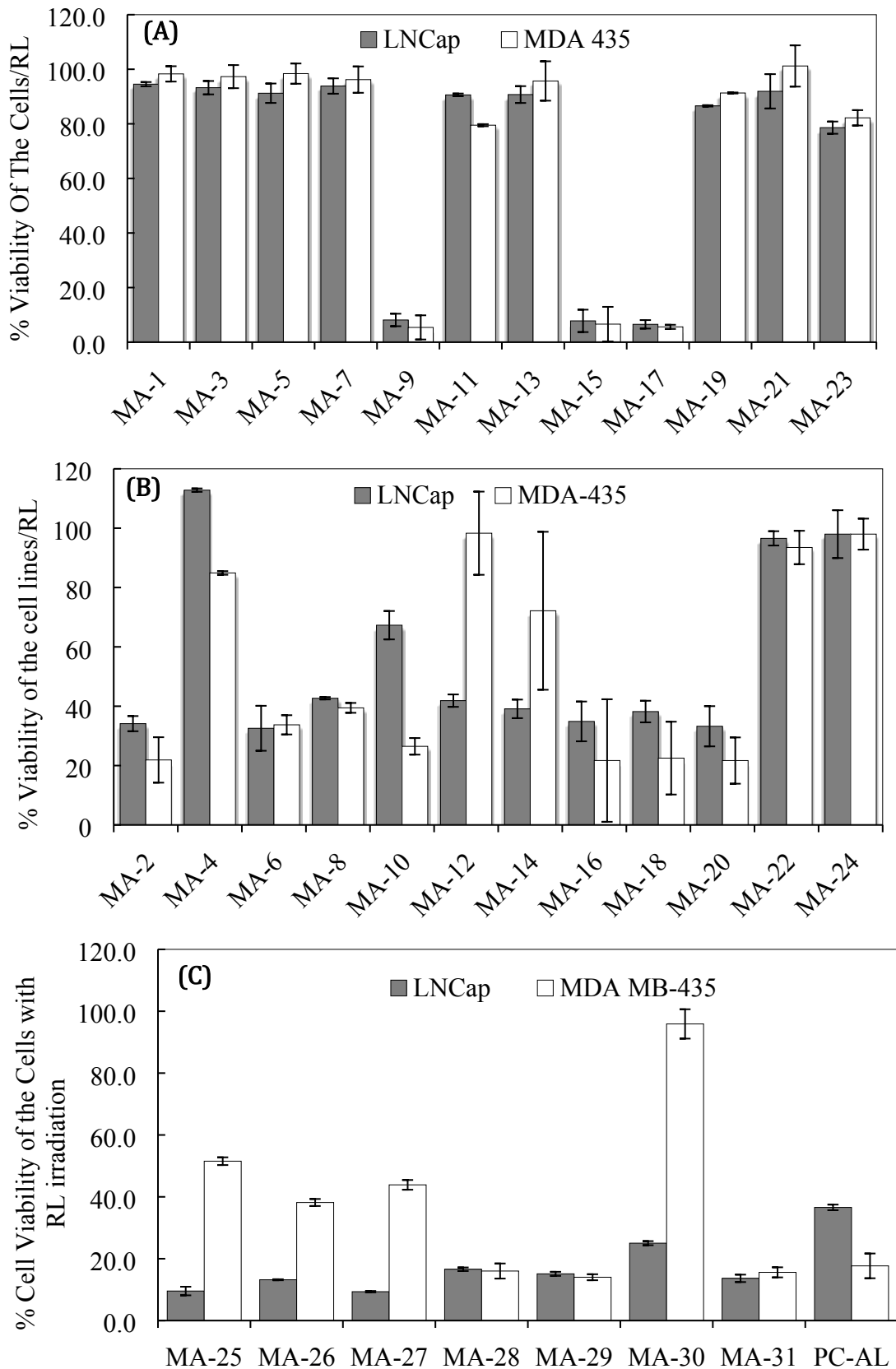
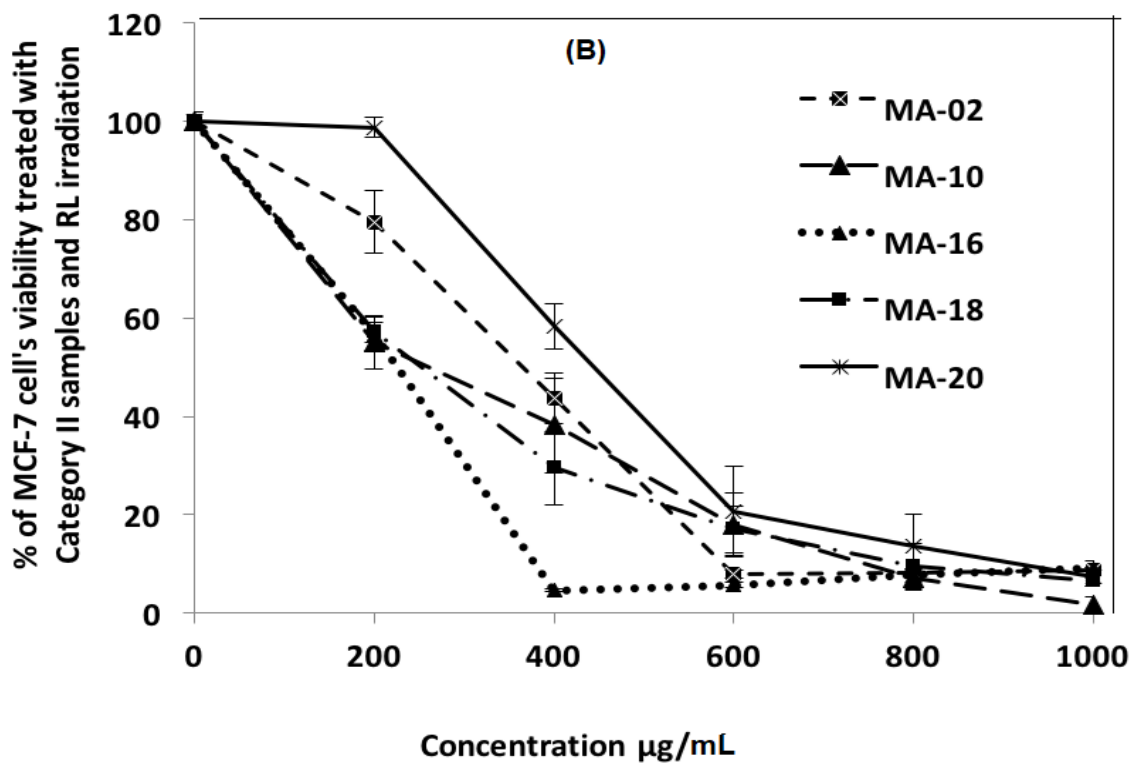
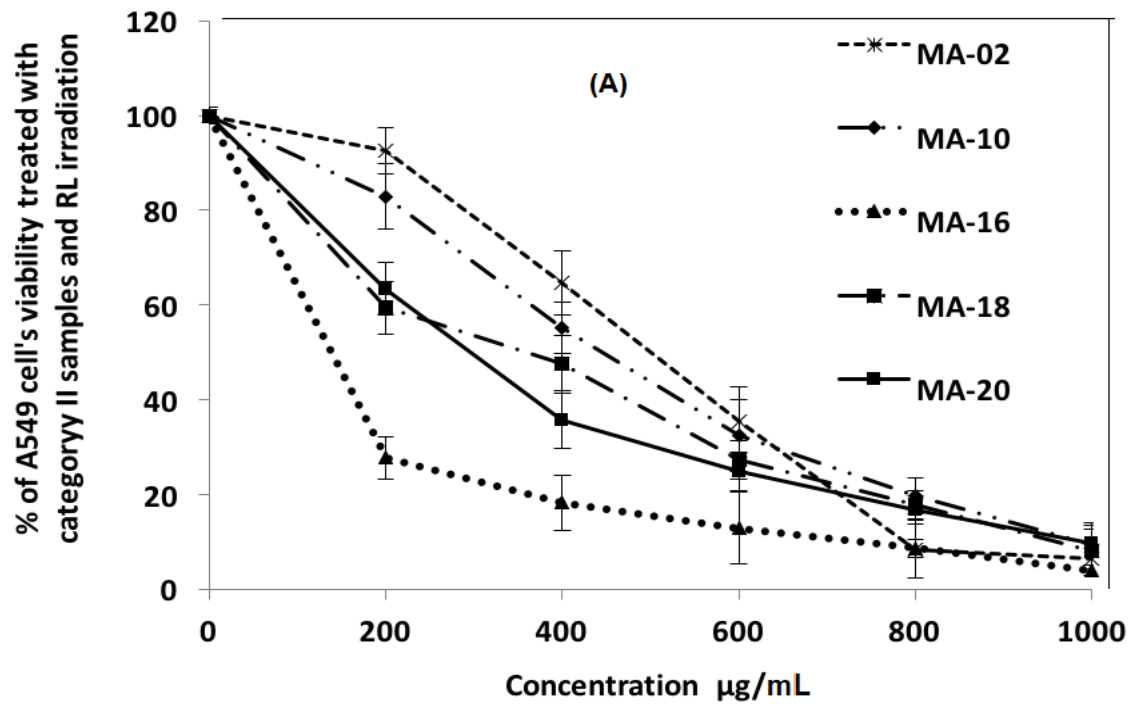


Figure S-3: Comparison of PDT effect of MA constituents on LNCap and MDA 435 viability with RL exposure. Cells were incubated with Category I and II. (500 $\mu\text{g}/\text{mL}$) and the plates were exposed to RL for 10 min. Error bars represent the standard deviation of three wells and $0.005 < P < 0.05$



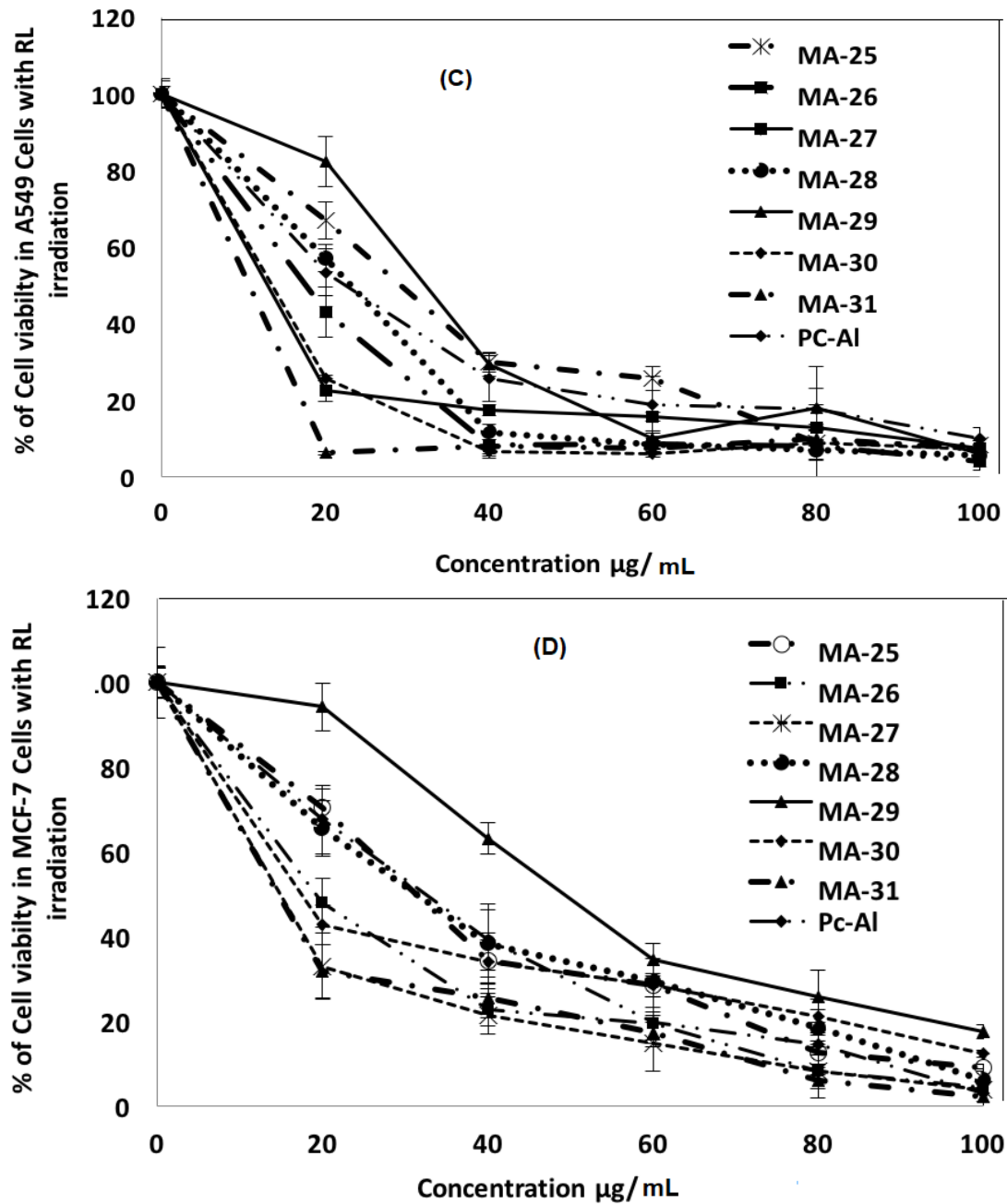


Figure S-4: Concentration effect of PDT of MA samples of (A and B) Category II and (C and D) Category III on (A) A549 and (B) MCF-7. The cells were exposed to RL for 10 min each. Error bars represent standard deviation